Bending Analysis of Hyperbolic Paraboloid Shells by Finite Element Method Using Thin Shallow Doubly Curved Elements

A Thesis Submitted
In Partial Fulfilment of the Requirements
for the Degree of
DOCTOR OF PHILOSOPHY

By
T. VENKATACHARYULU

to the

DEPARTMENT OF CIVIL ENGINEERING
INDIAN INSTITUTE OF TECHNOLOGY KANPUR
SEPTEMBER 1974

CERTIFICATE

This is to certify that the work entitled 'Bending Analysis of Hyperbolic Paraboloid Shells by Finite Element Method using Thin Shallow Doubly Curved Elements' by T. Venkatacharyulu has been carried out under my supervision and has not been submitted elsewhere for award of any degree.

P. Dayaratnam

(P. DAYARATNAM)
Professor
Department of Civil Engineering
Indian Institute of Technology
Kanpur.

ACKNOWLEDGEMENTS

The author wishes to express his appreciation for the guidance and encouragement given to this work by his thesis supervisor, Dr. P. D ayaratnam.

He is highly indebted to Dr. G.D. Agrawal for arranging his trip to I.I.T. Madras for computer work.

He would like to acknowledge, with deep thanks, the many fruitful discussions on this subject with Dr.P.N.Murthy and Dr. Y.C. Das.

Special thanks are due to Messers C.P. Vendhan and M. Hariharan and Dr. P. Purushottaman for their liberal assistance during the course of this work. He is grateful to Mr. M.S.R. Venkatachary for the unstinted and pains-taking help rendered in accomplishing the present achievement.

The author specially thanks Mr. K.N.Tewari for excellent typing of the manuscript.

He is thankful to his wife, Suresh, Ramesh, Kishore and Indu for bearing with him during the period of his work.

TABLE OF CONTENTS

LIST OF TABLES

LIST OF FIGURES

NOTATION

A	Middle surface area.
$[A]$	Matrix relating displacements and generalized displacements.
a,b	Projected dimensions of element in X and Y directions respectively.
$[A]_r$	Matrix relating rotations and generalized displacements.
$[B]_{S\ell}, [B]_{Sr}$. $[B]_b, [B]^*_{Sr}$	Strain transformation matrices.
$[C]_n$	Transformation matrix.
$[D], [D]_S, [D]_b$	Material, stretching and bending rigidity matrices.
$[e]$	Middle surface stretching deformation matrix.
$[e]_\ell, [e]_r$	Linear, nonlinear portions of $[e]$.
$[e]^0$	Initial stretching deformation matrix.
$\vec{i}_x$, $\vec{i}_y$, $\vec{i}_2$	Unit vectors acting in x,y,z directions.
$[k]$	Middle surface bending deformation matrix.
$[k]^0$	Initial bending deformation matrix
$[K]_n, [\bar{K}]_n$	Stiffness matrices for element n.
$[K]_{\ell,n}, [K]_{r,n}$	Linear, nonlinear portions of $[K]_n$
$[K]_{t,n}$	Tangential stiffness matrix for element n.
$[\bar{K}]_{g,n}$	Geometric stiffness matrix for element n.

$[k]_t$	System tangent stiffness matrix.
$[k]_\ell$	Linear system stiffness matrix.
$[K]_g$	Geometric system stiffness matrix.
$[M] = \{M_1, M_2, M_{12}\}$	Stress couple matrix.
$[N] = \{N_1, N_2, N_{12}\}$	Stress resultant matrix.
$\vec{n}$	Unit normal vector.
$[P]_n, [\bar{P}]_n$	Generalized force matrices for element n.
$[P]_{\ell,n}, [P]_{r,n}$	Linear, nonlinear portions of $[P]_n$.
p_1, p_2, p_n	Surface forces per unit area acting in ξ_1, ξ_2, ζ directions.
$[p]$	System generalized force matrix.
$1/R_{ij}$	Curvature measures.
$\vec{r}$	Position vector to middle surface.
S_j	Arc length along ξ_j parametric lines.
t	Thickness.
$\bar{t}_j$	Unit vector tangent to ξ_j curve.
u_1, u_2, w	Translations of middle surface in ξ_1, ξ_2, n directions.
$[U]_j$	Displacement matrix for node j.
$[U]_{E,n}$	Displacement matrix for element n.
$[u]$	System nodal displacement matrix.
V'	Strain energy per unit middle surface area.
X, Y, Z	Global cartesian directions.
α_j	Surface metrics.
$[\alpha]_n$	Matrix of generalized displacements for element n.

β_1, β_2	Rotations of normal toward ξ_1, ξ_2 directions.
$[\varepsilon]=\{\varepsilon_1, \varepsilon_2, \varepsilon_{12}\}$	Strain matrix at ξ_1, ξ_2, ζ.
$[\varepsilon]^0$	Initial strain matrix.
ζ	Thickness coordinate.
ξ_1, ξ_2	Curvilinear coordinates.
$[\sigma]=\{\sigma_1, \sigma_2, \sigma_{12}\}$	Stress matrix at ξ_1, ξ_2, ζ.
$[\omega]^*$	Rotation matrix.
R_1, R_2	Principal Radii of curvatures.

SYNOPSIS

BENDING ANALYSIS OF HYPERBOLIC PARABOLOID SHELLS BY FINITE ELEMENT METHOD USING THIN SHALLOW DOUBLY CURVED ELEMENTS

A Thesis Submitted
In Partial Fulfilment of the Requirements
For the Degree of
Doctor of Philosophy

by

T. VENKATACHARYULU

to the

Department of Civil Engineering
Indian Institute of Technology, Kanpur

SEPTEMBER 1974

The thesis presents development of the nonlinear differential equations both in stress function-vertical displacement (ϕ-w) and displacements in X-, Y- and Z-direction (u-v-w) forms for a hyperbolic paraboloid. As it is found difficult to solve them by analytical means, recourse has been taken to finite element method. The shell has been discretized into thin shallow doubly curved rectangular elements.

The stiffness matrix for a thin shallow doubly curved rectangular element with five degrees of freedom at each node has been generated by using numerical integration technique with 6-point Gauss-Legendre quadrature. This is independently checked by using a technique suggested by Kabaila.

The linear bending analysis using the above stiffness matrix has been applied to hyperbolic paraboloid shells bounded by ~~its~~ their characteristics under uniform vertical load for the following boundary conditions: (i) Simply supported and (ii) Clamped. The deflections, in-plane shears, bending moments etc., have been plotted for the various boundary conditions. The computer program which forms the most important tool in the finite element analysis has been developed independently. The convergence of results has been illustrated for 4x4, 6x6 and 8x8 mesh sizes of a hyperbolic paraboloidal shell with fixed edges carrying a uniform vertical load.

The nonlinear bending analysis for the case of large deflection (i.e. geometrically nonlinear) has been formulated and applied to a hyperbolic paraboloid shell with fixed edges under uniform vertical load using a 4x4 mesh size. The study has been confined to this particular mesh size in view of time and memory constraints on the computer. Newton-Raphson iteration has been adopted to trace the load-deflection curve at the centre of the shell. The tangent stiffness matrix and the geometric stiffness matrix have been generated by numerical integration technique by writing a special computer program. The buckling load for the shell has been indicated from the load-deflection behaviour and compared with the existing experimental results.

Four appendices have been provided to cover (i) numerical integration technique using Gauss-Legendre quadrature, (ii) computer integration of congruently transformed matrices due to Kabaila, (iii) stiffness matrix of straight beam with respect to eccentric axes and (iv) skewed boundary conditions.

CHAPTER 1

INTRODUCTION

1.1 GENERAL

Shallow doubly curved translational shells are efficient and aesthetically attractive structures and as such are being used extensively in roof construction. Due to the limited applicability of the membrane or 'momentless' theory, the bending theory of shells has received a great deal of attention in recent years (1,2,3,4,5,6)*.

The 'shallow shell theory' of Margeurre (1) and Vlasov (2) is often used as it is reasonably accurate for the shell dimensions used in practice and since it is considerably simplified in comparison with more accurate shell theories. The fundamental approximation of the shallo shell theory is that quadratic terms involving the slopes of the shell middle surface are negligible compared to unity. While there is certain uncertainty regarding the magnitudes of the errors introduced by the approximation, a common rule-of-thumb is that if the maximum rise/span ratio of the shell is less than one-fifth, the theory produces results sufficiently for practical purposes (83).

---

* Numbers in parentheses refer to references listed in the list of references.

The shallow shell theory is normally formulated in terms of either a stress function and normal displacement (ϕ-w) or in terms of middle-surface displacements u,v and w. The differential equations for both the above formulations have been derived for the large deflection case along with the boundary conditions. In the case of hyperbolic paraboloid, the harmonic functions do not suit because of the asymmetric relation between w and ϕ (7). Thus, despite the simplifying assumptions which are made, problem is still difficult one mathematically with the result that comparatively few analytical solutions have been obtained. A recent study (8) has quantitatively demonstrated the sensitivity of shells to boundary conditions thus emphasizing the importance of developing methods of analysis which are not restricted to special boundary conditions, particularly those specified by the simple support case. Evidently the most promising approach to the problem is a numerical one. Among the numerical procedures a distinction is often made between procedures which are regarded as mathematical approximations, such as finite differences and variational methods, and those which are physical approximations, such as various discrete element systems.

Das Gupta (9), Soare (10), Mirza (11), Russell and Gerstle (12,13) and others have presented finite difference solutions for the linear analysis of shallow shells particularly as related to various hyperbolic paraboloids

as bounded by characteristics. Abu-Sitta has applied finite difference methods to elliptic paraboloids (14).

In the application of the variational methods to the analysis of shallow shells (7), the problem of selection of approximating functions restricts the versatility of the method since a definite choice of such functions applies only to specific boundary conditions. In addition, the treatment of non-classical boundary conditions presents serious difficulties.

Among discrete element procedures which have been applied to shell problems are methods using the lumped parameter model (15,16), the framework or lattice model (17) and the finite element technique. While it is justified to classify the first two methods as physical idealizations*, in some applications ** the finite element approaches to plane stress (18) and plate bending (19,20) have met with notable success.

---

* The lumped parameter model may be regarded as a physical interpretation of finite difference approximations since the governing equations of the model are equivalent to the consistent difference equations of the problem. However, the model facilitates the formulation of boundary conditions without using fictitious grid points.

** The applications referred to are those in which the shape of the structure is not idealized. When, for example, flat elements are used to approximate a curved surface, a physical idealization is also involved.

A natural extension of the scope of the finite element method is to shell problems. Most of the early attempts to extend the method employed assemblages of flat elements to approximate the curved surface of the shell (21). Such an idealization may not be entirely satisfactory, however, since errors are introduced which are distinct from those involved in assuming the form of displacements in the structure (or element). Thus no direct relationship with the Rayleigh-Ritz procedure is apparent. Jones and Strome (22) demonstrated the need for the use of curved shell elements when solutions were sought for shells for revolution. Curved elements have been used for axisymmetric shells (23) and, for the cases that have been reported, more accurate results have been obtained than with flat elements. In the case of translational shells, the use of the doubly curved element gives more accurate result than that of flat element even for coarse mesh size. Since hoop stiffness present in shell of revolution problems is frequently not present in many translational shells, Schnobrich et al (21) are of the view that flat elements may be used for their analysis. This means that a curved surface is idealized as a folded plate. To derive a stiffness matrix for a completely general doubly curved shell element would be rather difficult because of the complicated differential geometry that would be involved and the operations on large size

matrices that would be required in the derivation. Because of this difficulty, Schnobrich et al (21) have gone in for flat triangular elements, in which there is no coupling between membrane stiffness and plate bending stiffness. This results in the simplicity of the derivation of the stiffness matrix making it possible to use higher order displacement functions to represent in-plane and bending displacements. If the number of elements which are used to represent the shell remains unchanged, using high order displacement functions for each element can efficiently improve the accuracy of the solution and the continuity of stresses between the elements. However, the corresponding increase in the number of generalized displacements in each element causes considerable increase in the number of simultaneous equations which have to be solved. This results in an increase in the band width and the computer storage capacity required. The computational effort becomes considerable and puts a serious limit on the number of elements which can be used. In this case, the advantages that can be gained by using higher order displacement functions tend to be destroyed by the poor geometri approximation growing out of the restriction on the number of elements that can be used. Thus, when effort is expanded on developing or choosing a flat shell element, it is important to consider the best balance between the displacement approximation and the geometric approximation.

Connor and Brebbia (24), Dhatt (25) and Pecknold and Schnobrich (26) have developed doubly curved finite elements using shallow shell theory and comparatively low order displacement functions. Use of curved elements for translational shells of constant curvature involves no geometric approximation.

1.2 REVIEW OF LITERATURE

As Kovach (27) puts it, it is necessary to analyse for the nonlinear phenomena that abound so widely in nature for clear understanding of the surrounding environment. The complexities of nonlinear analyses have created a 'non-linear barrier' which, only in very recent times, has begun to be penetrated through the efficient use of modern high speed computers. In structural mechanics, the unparalled success of the now well-known finite element method gives hope that the nonlinear barrier can, at last, be broken. Depending on the sources of nonlinearities, nonlinear problems can be divided into three categories. In brief, these categories are problems involving material nonlinearity alone, problems involving geometric nonlinearity alone, and problems involving both geometric and material nonlinearities.

1.2.1 Nonlinearities

Material nonlinearity is the easiest to visualise. It encompasses problems in which stresses are not linearly

proportional to the strains, but in which only small displacements and small strains are considered. Displacements refer to the changes in the overall geometry of the body whereas strains are related to internal deformations. The word 'small' usually implies infinitesimal changes in the geometry of the body. An example is elastic-plastic analysis of structures. Linear strain-displacement relations are used.

Geometric nonlinearity includes problems arising both from nonlinear strain-displacement relations and finite changes in geometry. Here linear stress-strain relations are used. In other words, this category encompasses large strains and large displacements. An important subclass of geometrically nonlinear problems is the case of small or infinitesimal strains and large or finite displacements. An example is the elastic post-buckling behaviour of structures.

Finally, the third and most general category of nonlinear problems is the combination of the first two categories. It involves nonlinear constitutive behaviour as well as large strains and finite displacements. The deformation of a rubber like material is an example of the third category.

In large span shells, it becomes necessary to cut down the weight of the structure by making the shell thin. This necessitates the analysis of shells for large

deflection taking the strains as small. Similarly the aircraft and ship structures are designed. The above come under the problems of geometric nonlinearity which is now reviewed.

1.2.2 Geometrically Nonlinear Analysis

Various surveys of the present topic have appeared in recent years. Martin (28), gave a thorough review of all work in geometrically nonlinear finite element analyes upthrough 1969, the present review begins from there onwards. Oden (29) gave a correspondingly thorough assessment that covered a wide range of nonlinearities, including material nonlinearities and many special forms of higher-order nonlinearities (e.g., large strains) which are excluded from the present review. Stricklin and his associates at the Sandia Corporation have contributed a great deal to the present topic in recent years (30).

The formulation of element force-displacement equations for geometrically nonlinear analysis can be approached from many standpoints. The attention is restricted to the concept of stationary potential energy and to a Lagrangian discription of behaviour, i.e., displaced points are referred to a fixed set of axes.

The typical governing equation of geometric nonlinear problem in indicial form is

$$P_i = N_{ij}\,\Delta_j + \tfrac{1}{2}N_{ijk}\,\Delta_j\,\Delta_k + \tfrac{1}{3}N_{ijk\ell}\,\Delta_j\,\Delta_k\,\Delta_\ell \qquad (1.1a)$$

or, in matrix form

$$\{P\} = [K]\{\Delta\} + [N_1(\Delta)]\{\Delta\} + [N_2(\Delta)]\{\Delta\} \qquad (1.1b)$$

where $[K]$ is the usual linear stiffness matrix,

and $[N_1]$ and $[N_2]$ are the first- and second-order 'geometric' or 'incremental' stiffness matrices respectively.

The elements of $[N_1]$ are linear functions of the displacements while the elements of $[N_2]$ are quadratic functions of the displacements. Thus, the above formulation ends up in the solution of nonlinear equations. The parameters to be solved for differ from one physical circumstance to another and they do not pertain exclusively to a tracing of the load-displacement response along a continuous curve, starting from the linear regime at small loads onto significant nonlinearities at higher loads. According to Gallagher and Mau (36), three areas of interest with respect to algorithmic tools are perceived: (1) general nonlinear analysis with reference to bifurcation phenomena, (2) calculation of bifurcation or 'branching' points and (3) determination of the load-displacement response along a post-buckling path.

1.2.3 General Nonlinear Analysis

General nonlinear analysis using procedures which operate directly on the potential energy have two advantages Firstly, the representation of the system can be conveniently

established without recourse to large-scale matrix operations, since energy is a scalar. Secondly, it had been hoped that the calculation of a stationary value for a more general nonlinear function might not be significantly more difficult than that for a quadratic function. Bogner, Fox and Schmit (33) used function minimization procedures in nonlinear finite element analysis. It has been claimed that the energy search method may be used effectively for the geometric nonlinear analysis. Unfortunately, other researchers (for example, Oden and Key (34)) have reported disappointing results with the energy search method. Computational experience has not proved conclusively that the advantages of directly operating on the potential energy are indeed manifested in application. A view of the function minimization schemes is given by Broyden (35), but without reference to physical applications.

Methods which attack directly the solution of the governing equilibrium equations are overwhelmingly the most popular in application to geometrically nonlinear analysis. Many different specific forms are available, including direct iteration, Newton-Raphson, incremental and initial value methods. In discussing these methods, it must be borne in mind that in tracing a load-displacement response through a significant range of nonlinear behaviour, it is essential to deal with intervals of loading, the solution for an interval being employed as the starting data for the

second interval. Numerical calculation shows that it is not possible, in general, to proceed from the unloaded to final state in a single step due to numerical instabilities in the solution.

1.2.4 Solution by Direct Iteration

Direct iteration is seemingly the most attractive approach to geometrically nonlinear analysis since it requires only the inversion (or solution) of the linear portion of the governing equations. The iterative sequence for the solution continues until the difference between two successive solutions converges to a specified tolerance. Convergence difficulties are encountered when the nonlinearities are severe. Such difficulties are often manifested by continued iteration in a loop about the convergent solution. In such cases an improved procedure is to employ a higher order iterative scheme as described by (36). The approach, in any case, suffers from inefficiency in comparison with certain alternatives. To improve this situation, Roberts and Ashwell (37) form the right hand side with use of an estimated mid-increment displacement field.

1.2.5 Newton-Raphson Method

Direct iteration can be interpreted as an approximate form of the Newton-Raphson method. To explain this

approach, all the nonlinear terms of the potential energy are indicated by π_{NL}. Stricklin, et al (30) have shown that this method is of the form

$$([K] + \frac{\partial^2 \pi_{NL}}{\partial \Delta_i \partial \Delta_j})\delta \Delta = -[K]\{\Delta^0\} - \{\frac{\partial \pi_{NL}}{\partial \Delta}\} + \{P\} \qquad (1.2)$$

where π_{NL} is formed on the basis of $\{\Delta^0\}$ and $\{\delta \Delta\}$ symbolises the displacement interval covered by the iterative process. The solution for $\{\delta \Delta\}$ is used to improve $\{\Delta^0\}$ and the process is continued until $\{\delta \Delta\}$ is sufficiently close to zero. From the efficiency standpoint, a major difficulty in the Newton-Raphson approach is the need to reform the matrix on the left hand side and to invert it or solve the equations in each iteration. Also the step size for each solution is very critical since the method will not converge unless it is sufficiently close to the solution point. The method possesses second-order convergence properties. The Newton-Raphson scheme may be modified to eliminate or minimize the repeated matrix inversion.

1.2.6 Incremental Method

The incremental method is probably the most widely-used of the procedures addressed directly to the solution of the equilibrium equations. It has been given a theoretical footing in the variational context by many authors, e.g. Hofmeister, et al (38), Pian and Tong (39) and Fellippa (40). In this, a tangent stiffness is

constructed for the interval in question and the solution for the interval begins with the solution of the prior interval as a base. Stricklin, et al (30) and Zienkiewicz and Nayak (41) also discussed about the same. Dupuis, Pfaffinger and Marcal (42) have made effective use of incremental method in shell applications, where initial imperfections are of considerable importance.

1.2.7 Perturbation Method

Walker (43) and Morin (44) have applied the perturbation approach to nonlinear analysis. Their results demonstrate the desirability of a corrector step, e.g., Newton-Raphson iteration. Although perturbation concepts show no particular advantage in this type of analysis, they are especially important in post-buckling analysis.

1.2.8 Buckling Analysis

The bifurcation (buckling) analysis is founded on the assumption that the distribution of internal forces in the structure, due to applied loads which cause bifurcation, can be computed using linear analysis. This procedure is, therefore, termed linear stability analysis. The second variation of the potential energy is zero for bifurcation (neutral equilibrium). Thus conservative loading is implied. Only a limited amount of work has been reported on problems of finite element elastic instability

analysis for non-conservative loadings (45). Contributions to finite element eigenvalue analysis on the iterative side have recently been made by Bronlund (46), Whetstone and Jones (47), Rosen and Rubenstein (48) and Dong et al (49). Method of conjugate gradients (50) has been applied to eigenvalue determination.

The perturbation method and its variants constitute, almost exclusively, the approach to tracing load-displacement behaviour along the post-bifurcation branch.

Geometrically nonlinear finite element analysis is on a sound theoretical footing. The basic relationships are generally accepted, many different plate and shell elements are capable of formulation for such analysis and solution algorithms abound. Computational efficiency and reliability are questionable areas, however. Disproportionately small efforts have been devoted to reducing solution costs. The work of Stricklin and his colleagues (30) is among the exceptions.

The above review limits attention to procedures in which updating of structural geometry is not a critical aspect of the problems solved by these procedures. The work of Murray and Wilson (53) and allied developments are based upon the updating of geometry. Such updating is of course useful in enhancing the computational efficiency for moderate nonlinearities and is essential when the

nonlinearity is severe. Reference (30) studies the limitations of the subject procedures in this regard.

Perhaps the most important class of practical problems for which geometric nonlinearity is important is that concerned with elastic instability. A hierarchy of finite element approaches to this problem is taking form. At one end of the scale is the simple approach of linear stability analysis. This approach gives an overestimate to the strength of imperfection sensitive structures. Almroth and Brogan (54) have very recently shown that equally serious underestimates are given for cases where sensitivity to initial imperfection is not a factor in the determination of the limit load. At the other end of the scale are problems governed by higher-order terms in the geometric nonlinearities and material nonlinearities. The papers by Oden (55) and Stricklin, Haisler and Von Riesemann (56) define well the current status of finite element approaches to their solution.

1.2.9 Use of Hybrid Elements

In 1964, Pian (72) suggested a method which was later discussed more rigorously by Pian and Tong (73) in which the interelement boundary displacement compatibility can be satisfied rather easily. In this approach, one assumes an equilibrium stress field in the interior of the element, and a displacement field at the boundary of the element, which inherently satisfies the interelement

compatibility condition. Pian's approach has since been employed in several small-deflection elastic problems such as plate bending, shell problems and analysis of multi-layered plates and shells where transverse shear effect is important. They clearly demonstrated the versatility of the hybrid stress model for deriving stiffness matrices of elements of arbitrary geometry.

Using the above approach, some satisfactory results were obtained for incremental analysis of large deflection problems by Pirotin (74). As discussed by Pian (75), these methods cannot be considered as being based on the modified complementary energy principle which is the basis of the hybrid stress model and hence cannot be considered as consistent hybrid stress finite element methods.

Since, as discussed by Pian (75), the hybrid assumed stress finite element model has proved to be more versatile structural tool, it is necessary to present a consistent variational formulation of the hybrid stress model for the incremental analysis of large deflection problems. The concept of initial stress is to be employed, wherein, during any given step in which the displacements, stresses and external loads undergo increments, the state at the beginning of the step is considered as one of initial stress. A 'check' on the equilibrium in the state prior to the addition of further load increment is to be included.

Since the hybrid stress model (76) has proven to be a valuable tool in the linear analysis of complex problems such as sandwich plates and shells and problems with singularities, it can be expected to be of equal value in large deflection problems.

1.3 BASIC EQUATIONS

The objective is to develop the nonlinear differential equations for thin shallow shells having large deflection. The equations are specialized for a hyperbolic paraboloid bounded by elastic edge beams along the characteristics.

1.3.1 General

Medium bending of shell is defined (57) as that when the maximum deflection is of the same order as thickness or larger, but is small in comparison with other linear dimensions of the shell. As the shell is shallow, the effects of tangential displacements on rotations and change of curvatures is neglected. The assumptions of the shallow shell theory are:

(A) The shell or plate is thin so that shear deformation is neglected.

(B) Kirchhoff's hypothesis is accepted, i.e., normal stresses perpendicular to the middle surface are neglected and normal to the middle surface does not undergo any deformation.

(C) Medium bending of shell is considered.

(D) The squares of elongations and shears and the products of elongations and rotations are neglected. The rotation about Z-axis is neglected. The squares of rotations about α_1 and α_2 which are of the order of elongations and shear are retained.

(E) A shell is considered shallow when the rise to span (smaller) ratio is less than 1/5. Also $L^2/R_1R_2 \ll 1$ where L is the bigger span.

(F) In the case of shallow shells, Love's first approximation is used, i.e., $(1+k_1Z) \simeq (1+k_2z) \simeq 1$.

The quadratic terms involving the slopes of the shell middle surface are negligible compared to unity. If the shell middle surface is a second order surface, this assumption leads directly to the approximation that the curvatures of the middle surface are constant. An additional consequence is that the geometry of the surface is, in effect, approximated by that of its projection on the horizontal plane. Thus, if the parametric representation of the shell middle surface is given in the form

$$\begin{aligned} X &= X \\ Y &= Y \\ Z &= Z(X,Y) \end{aligned} \qquad (1.3)$$

where (X,Y,Z) are cartesian coordinates, the approximation is made that the (X,Y) coordinate lines are orthogonal on the middle surface. It is in this sense that the term 'orthogonal coordinates' will be used throughout the remainder of this study.

(G) Gauss-Codazzi equations hold good for the continuity of the surface.

1.3.2 Strain-Displacement Relations in Orthogonal Curvilinear Coordinates

Let α_i and k_{ij} be the quantities which characterize the middle surface of the shell before deformation, referred to orthogonal curvilinear coordinates ξ_1, ξ_2. During manufacturing and erecting of the shell, initial deformations occur invariably. The irregularities may appear prior to the application of the load or owing to non-uniform temperature distribution in the shell. Initial stresses may also appear. These lead to deviation from orginal surface. It is assumed that the new surface is also shallow, so that the effect of tangential displacements on the initial rotations and the changes of curvature may be neglected. The superscript '0' refers to initial deformations.

$$
\begin{aligned}
\omega_1^0 &= \frac{1}{\alpha_1} \frac{w^0}{\xi_1} \\
\varepsilon_{11}^0 &= e_{11}^0 + \frac{1}{2}\omega_1^{0\,2} \\
2\varepsilon_{12}^0 &= e_{12}^0 + e_{21}^0 + \omega_1^0 \omega_2^0 \\
\chi_{11}^0 &= \frac{1}{\alpha_1 \alpha_2}\left(-\alpha_2 \frac{\partial \omega_1^0}{\partial \xi_1} - \omega_2^0 \frac{\partial \alpha_1}{\partial \xi_2}\right) \\
\chi_{12}^0 &= \frac{1}{\alpha_1 \alpha_2}\left(-\alpha_2 \frac{\partial \omega_2^0}{\partial \xi_1} + \omega_1^0 \frac{\partial \alpha_1}{\partial \xi_2}\right)
\end{aligned}
\qquad (1.4)
$$

where

$$e_{11}^{0} = \frac{1}{\alpha_1}\frac{\partial u_1^{0}}{\partial \xi_1} + \frac{1}{\alpha_1\alpha_2}\frac{\partial \alpha_1}{\partial \xi_2}u_2^{0} + k_{11}w^{0}$$

$$e_{12}^{0} = \frac{1}{\alpha_1}\frac{\partial u_2^{0}}{\partial \xi_1} - \frac{1}{\alpha_1\alpha_2}\frac{\partial \alpha_1}{\partial \xi_2}u_1^{0} + k_{12}w^{0} \qquad 1 \rightleftarrows 2$$

The elongations and rotations due to surface load may be determined by the following formulae (57)

$$\omega_1 = \frac{1}{\alpha_1}\frac{\partial w}{\partial \xi_1}$$

$$\varepsilon_{11} = e_{11} + \frac{1}{2}\omega_1^{2} + \omega_1^{0}\omega_1$$

$$= \frac{1}{\alpha_1}\frac{\partial u_1}{\partial \xi_1} + \frac{1}{\alpha_1\alpha_2}\frac{\partial \alpha_1}{\partial \xi_2}u_2 + k_{11}w + \frac{1}{2}\left(\frac{1}{\alpha_1}\frac{\partial w}{\partial \xi_1}\right)^{2}$$

$$+ \left(\frac{1}{\alpha_1}\frac{\partial w^{0}}{\partial \xi_1}\right)\left(\frac{1}{\alpha_1}\frac{\partial w}{\partial \xi_1}\right) \qquad (1.5)$$

$$2\varepsilon_{12} = e_{12} + e_{21} + \omega_1\omega_2 + \omega_1^{0}\omega_2 + \omega_2^{0}\omega_1$$

$$= \frac{1}{\alpha_1}\frac{\partial u_2}{\partial \xi_1} - \frac{1}{\alpha_1\alpha_2}\frac{\partial \alpha_1}{\partial \xi_2}u_1 + k_{12}w$$

$$+ \frac{1}{\alpha_2}\frac{\partial u_1}{\partial \xi_2} - \frac{1}{\alpha_1\alpha_2}\frac{\partial \alpha_2}{\partial \xi_1}u_2 + k_{21}w$$

$$+ \frac{1}{\alpha_1\alpha_2}\frac{\partial w}{\partial \xi_1}\frac{\partial w}{\partial \xi_2} + \frac{1}{\alpha_1\alpha_2}\frac{\partial w^{0}}{\partial \xi_1}\frac{\partial w}{\partial \xi_2} + \frac{1}{\alpha_1\alpha_2}\frac{\partial w^{0}}{\partial \xi_2}\frac{\partial w}{\partial \xi_1}$$

$$\chi_{11} = -\frac{1}{\alpha_1}\frac{\partial}{\partial \xi_1}\left(\frac{1}{\alpha_1}\frac{\partial w}{\partial \xi_1}\right) - \frac{1}{\alpha_1\alpha_2^{2}}\frac{\partial \alpha_1}{\partial \xi_2}\frac{\partial w}{\partial \xi_2}$$

$$\chi_{12} = -\frac{1}{\alpha_1}\frac{\partial}{\partial \xi_1}\left(\frac{1}{\alpha_2}\frac{\partial w}{\partial \xi_2}\right) + \frac{1}{\alpha_1^{2}\alpha_2}\frac{\partial w}{\partial \xi_1}\frac{\partial \alpha_1}{\partial \xi_2} \qquad 1 \rightleftarrows 2$$

The projections of the total displacements, the corresponding elongations and the changes of curvature will be summation of the quantities owing to initial deformations and the corresponding quantities due to load.

1.3.3 Derivation of Equilibrium Equations in Orthogonal Curvilinear Coordinates

If the stresses appearing in the shell during the manufacture and assembly are removed, but the initial deformation remains, then the irregularities are residual and that they appear as single normal displacement using $u_1^0 = u_2^0 = 0$.

The equations for the state of equilibrium of the shell under the normal load are derived using Reissner's variational theorem. The elongationsat any point 'Z' from the middle surface are given by the following:

$$\begin{aligned} \varepsilon_1 &= \varepsilon_{11} + Z\chi_{11} \\ \varepsilon_2 &= \varepsilon_{22} + Z\chi_{22} \\ \gamma_{12} &= 2\varepsilon_{12} + Z(\chi_{12} + \chi_{21}) \end{aligned} \tag{1.6}$$

The expressions for the components of stresses at any point 'Z' from the middle surface of the shell are as below:

$$\begin{aligned} \sigma_1 &= \frac{N_1}{t} + \frac{M_1 Z}{t^3/12} \\ \sigma_2 &= \frac{N_2}{t} + \frac{M_2 Z}{t^3/12} \end{aligned} \tag{1.7}$$

$$\tau_{12} = \frac{N_{12}}{t} + \frac{M_{12}Z}{t^3/12}$$

where N_1, N_2, N_{12} are stress resultants and M_1, M_2, M_{12} are stress couples.

The variational equation may be written as

$$\delta[\iiint \{ \sigma_1\varepsilon_1 + \sigma_2\varepsilon_2 + \tau_{12}\gamma_{12} - \frac{1}{2E}(\sigma_1^2 + \sigma_2^2) - 2\nu\,\overline{\sigma_1+\sigma_2} + 2\,\overline{1+\nu}\;\tau_{12}^2\}\,\alpha_1\alpha_2\, d\xi_1\, d\xi_2\, dZ - \iint P_N\, w\, \alpha_1\alpha_2\, d\xi_1\, d\xi_2] = 0 \qquad (1.8)$$

Substituting for the quantities in the above, the variation is carried out with respect to the unknowns u_1, u_2, w, N_1, N_2, N_{12}, M_1, M_2 and M_{12}. Since δu_1, δu_2, δw, δN_1, δN_2, δN_{12}, δM_1, δM_2 and δM_{12} are arbitrary, the coefficients of each must be zero. The above gives three equilibrium equations in u_1, u_2 and w directions and six force-displacement relations along with proper boundary conditions.

$$\frac{\partial}{\partial\xi_1}(N_1\alpha_2) + \frac{\partial}{\partial\xi_2}(N_{12}\alpha_1) - N_2\frac{\partial\alpha_2}{\partial\xi_1} + N_{12}\frac{\partial\alpha_1}{\partial\xi_2} = 0$$

$$\frac{\partial}{\partial\xi_1}(N_{12}\alpha_2) + \frac{\partial}{\partial\xi_2}(N_2\alpha_1) - N_1\frac{\partial\alpha_1}{\partial\xi_2} + N_{12}\frac{\partial\alpha_2}{\partial\xi_1} = 0$$

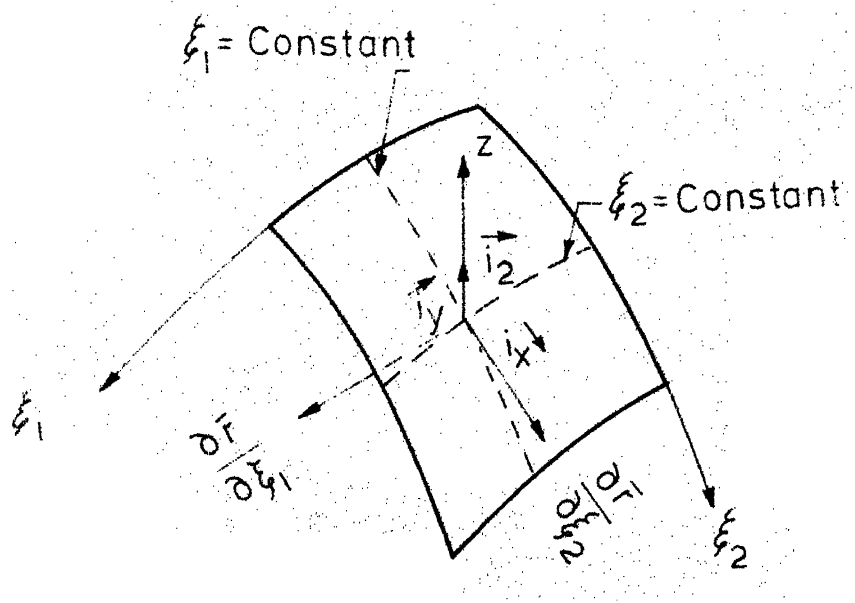

FIG. 1.1 COORDINATE VECTORS

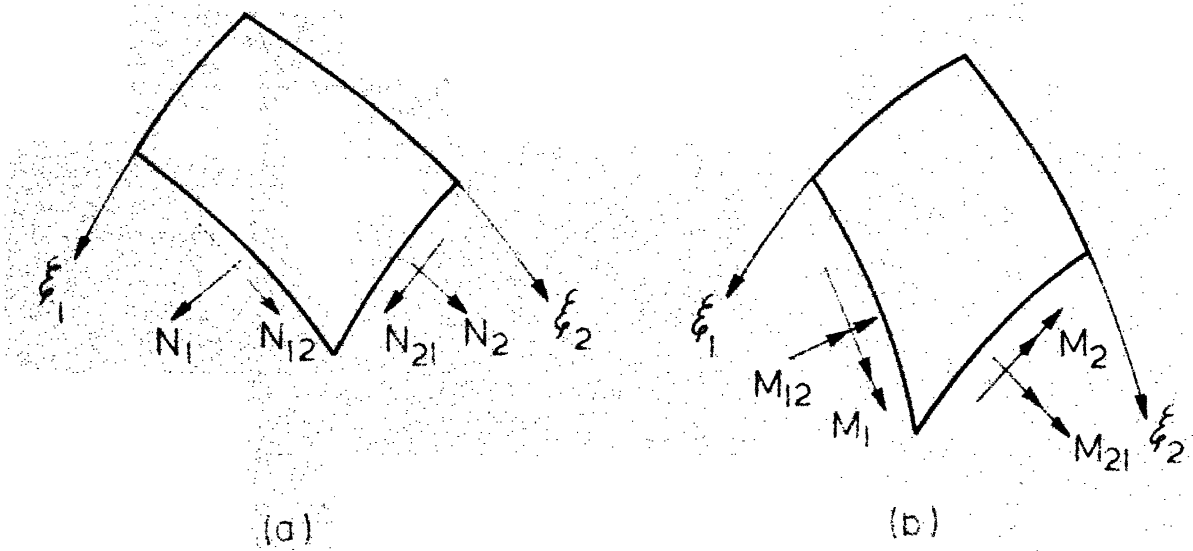

FIG. 1-2 THE POSITIVE DIRECTIONS OF STRESS RESULTANTS AND STRESS COUPLES

$$\frac{\partial^2}{\partial \xi_1^2}\left(M_1 \frac{\alpha_2}{\alpha_1}\right) + 2\frac{\partial^2}{\partial \xi_1 \partial \xi_2}(M_{12}) + \frac{\partial^2}{\partial \xi_2^2}\left(M_2 \frac{\alpha_1}{\alpha_2}\right)$$

$$+ \frac{\partial}{\partial \xi_1}\left(N_1 \frac{\alpha_2}{\alpha_1} \frac{\partial w}{\partial \xi_1}\right) + \frac{\partial}{\partial \xi_1}\left(N_1 \frac{\alpha_2}{\alpha_1} \frac{\partial w^0}{\partial \xi_1}\right)$$

$$+ \frac{\partial}{\partial \xi_2}\left(N_2 \frac{\alpha_1}{\alpha_2} \frac{\partial w}{\partial \xi_2}\right) + \frac{\partial}{\partial \xi_2}\left(N_2 \frac{\alpha_1}{\alpha_2} \frac{\partial w^0}{\partial \xi_2}\right)$$

$$+ \frac{\partial}{\partial \xi_2}\left(N_{12} \frac{\partial w}{\partial \xi_1}\right) + \frac{\partial}{\partial \xi_1}\left(N_{12} \frac{\partial w}{\partial \xi_2}\right)$$

$$+ \frac{\partial}{\partial \xi_2}\left(N_{12} \frac{\partial w^0}{\partial \xi_1}\right) + \frac{\partial}{\partial \xi_1}\left(N_{12} \frac{\partial w^0}{\partial \xi_2}\right) \qquad (1.9)$$

$$+ \frac{\partial}{\partial \xi_1}\left(M_1 \frac{\alpha_2}{\alpha_1^2} \frac{\partial \alpha_1}{\partial \xi_1}\right) + \frac{\partial}{\partial \xi_2}\left(M_2 \frac{\alpha_1}{\alpha_2^2} \frac{\partial \alpha_2}{\partial \xi_2}\right)$$

$$- \frac{\partial}{\partial \xi_1}\left(\frac{M_2}{\alpha_1} \frac{\partial \alpha_2}{\partial \xi_1}\right) - \frac{\partial}{\partial \xi_2}\left(\frac{M_1}{\alpha_2} \frac{\partial \alpha_1}{\partial \xi_2}\right)$$

$$+ 2\frac{\partial}{\partial \xi_1}\left(\frac{M_{12}}{\alpha_1} \frac{\partial \alpha_1}{\partial \xi_2}\right) + 2\frac{\partial}{\partial \xi_2}\left(\frac{M_{12}}{\alpha_2} \frac{\partial \alpha_2}{\partial \xi_1}\right)$$

$$- \alpha_1 \alpha_2 \{N_1 k_{11} + N_2 k_{22} + N_{12}(k_{12} + k_{21})\} + \alpha_1 \alpha_2 P_N = 0$$

The force-displacement relations are the standard ones and hence are not repeated here.

1.3.4 Reduction to a System of Two Nonlinear Equations

A force function $\emptyset$ is introduced which will satisfy the first two equilibrium equations of (1.9).

$$N_1 = \frac{1}{\alpha_2}\frac{\partial}{\partial \xi_2}\left(\frac{1}{\alpha_2}\frac{\partial \phi}{\partial \xi_2}\right) + \frac{1}{\alpha_1^2 \alpha_2}\frac{\partial \alpha_2}{\partial \xi_1}\frac{\partial \phi}{\partial \xi_1}$$

$$N_2 = \frac{1}{\alpha_1}\frac{\partial}{\partial \xi_1}\left(\frac{1}{\alpha_1}\frac{\partial \phi}{\partial \xi_1}\right) + \frac{1}{\alpha_1 \alpha_2^2}\frac{\partial \alpha_1}{\partial \xi_2}\frac{\partial \phi}{\partial \xi_2} \qquad (1.10)$$

$$N_{12} = \frac{1}{\alpha_1 \alpha_2}\left[- \frac{\partial^2 \phi}{\partial \xi_1 \partial \xi_2} + \frac{1}{\alpha_2}\frac{\partial \alpha_2}{\partial \xi_1}\frac{\partial \phi}{\partial \xi_2} + \frac{1}{\alpha_1}\frac{\partial \phi}{\partial \xi_1}\frac{\partial \alpha_1}{\partial \xi_2}\right]$$

After introducing equations (1.10) in the first two equations of (1.9), the left hand side of the two equations of (1.9) becomes

$$- \frac{\alpha_1 \alpha_2}{R_1 R_2}\frac{1}{\alpha_1}\frac{\partial \phi}{\partial \xi_1} \qquad \vec{1}, 2 \qquad (1.11)$$

which can be neglected for shallow shell with non-zero Gaussian curvature and is zero for shells of zero Gaussian curvature.

Also,

$$N_1 + N_2 = \nabla^2 \phi \qquad (1.12)$$

where operator ∇^2 is defined as

$$\nabla^2 = \frac{1}{\alpha_1 \alpha_2}\left[\frac{\partial}{\partial \xi_1}\left(\frac{\alpha_2}{\alpha_1}\frac{\partial}{\partial \xi_1}\right) + \frac{\partial}{\partial \xi_2}\left(\frac{\alpha_1}{\alpha_2}\frac{\partial}{\partial \xi_2}\right)\right] \qquad (1.13)$$

A system of two nonlinear equations can be obtained in ϕ and w from Gauss equation of continuity of deformation and third equilibrium equation (1.9). Gauss equation of continuity of deformation becomes

$$\frac{\partial}{\partial \xi_1}\left[-\frac{1}{\alpha_1}\left\{\frac{\partial}{\partial \xi_1}(\alpha_2 \varepsilon_{22}) - \varepsilon_{11}\frac{\partial \alpha_2}{\partial \xi_1} - \frac{\partial}{\partial \xi_2}(\alpha_1 \varepsilon_{12}) - \varepsilon_{12}\frac{\partial \alpha_1}{\partial \xi_2}\right\}\right]$$

$$+ \frac{\partial}{\partial \xi_2}\left[-\frac{1}{\alpha_2}\left\{\frac{\partial}{\partial \xi_2}(\alpha_1 \varepsilon_{11}) - \varepsilon_{22}\frac{\partial \alpha_1}{\partial \xi_2} - \frac{\partial}{\partial \xi_1}(\alpha_1 \varepsilon_{12}) - \varepsilon_{12}\frac{\partial \alpha_2}{\partial \xi_1}\right\}\right]$$

$$= Et[\chi_{12}^2 + 2\chi_{12} k_{12}^0 - \chi_{11}(k_{22}^0 + \chi_{22}) - \chi_{22} k_{11}^0] \qquad (1.14)$$

$$= \nabla^2(N_1 + N_2)$$

or

$$\nabla^2\nabla^2 \phi - Et[\chi_{12}^2 + 2\chi_{12} k_{12}^0 - \chi_{11}(k_{22}^0 + \chi_{22}) - \chi_{22} k_{11}^0] = 0 \qquad (1.15)$$

where $k_{ij}^0 = k_{ij} + \chi_{ij}^0$

The third equilibrium equation is reduced to an equation in w and ϕ as follows:

$$D \nabla^2 \nabla^2 w + N_1 K_{11} + N_2 K_{22} + 2N_{12} K_{12} - P_N = 0 \qquad (1.16)$$

where $K_{ij} = k_{ij} + \chi_{ij}^0 + \chi_{ij}$

In the further analysis, initial deformations are not considered. In that case, the more general one, when the coordinate lines are not the lines of principal curvature, takes intoaccount the twisting of the surface and the two fundamental equations become

$$\frac{1}{Eh}\nabla^4\phi - \{\left(\frac{\partial^2 w}{\partial\xi_1\partial\xi_2}\right)^2 - \frac{\partial^2 w}{\partial\xi_1^2}\frac{\partial^2 w}{\partial\xi_2^2} - k_1\frac{\partial^2 w}{\partial\xi_2} - k_2\frac{\partial^2 w}{\partial\xi_1^2} + 2t\frac{\partial^2 w}{\partial\xi_1\partial\xi_2}\}$$

$$= 0$$

$$D\nabla^4 w - \left(k_2\frac{\partial^2\phi}{\partial\xi_1} + k_1\frac{\partial^2\phi}{\partial\xi_2^2} - 2t\frac{\partial^2\phi}{\partial\xi_1\partial\xi_2}\right) \qquad (1.17)$$

$$- \left(\frac{\partial^2\phi}{\partial\xi_2^2} - 2\frac{\partial^2\phi}{\partial\xi_1\partial\xi_2}\frac{\partial^2 w}{\partial\xi_1\partial\xi_2} + \frac{\partial^2\phi}{\partial\xi_1^2}\frac{\partial^2 w}{\partial\xi_2^2}\right) - P_N = 0$$

If the equation of the middle surface of a shallow shell has been assigned as $Z = Z(\xi_1, \xi_2)$, then it is possible to calculate approximate curvatures by using the approximate formulas

$$k_1 = \frac{\partial^2 Z}{\partial\xi_1^2}$$

$$k_2 = \frac{\partial^2 Z}{\partial\xi_2^2} \qquad (1.18)$$

$$t = \frac{\partial^2 Z}{\partial\xi_1\partial\xi_2}$$

When the coordinate lines become the lines of principal curvature, the twist term disappears and the fundamental differential equations of nonlinear shell theory become

$$\frac{1}{Eh}\nabla^4\phi - \{\left(\frac{-\partial^2 w}{\partial\xi_1\partial\xi_2}\right)^2 - \frac{\partial^2 w}{\partial\xi_1^2}\frac{\partial^2 w}{\partial\xi_2^2} + k_2\frac{\partial^2 w}{\partial\xi_1^2} + k_1\frac{\partial^2 w}{\partial\xi_2^2}\} = 0$$

$$D\nabla^4 w + \left(k_2\frac{\partial^2\phi}{\partial\xi_1^2} + k_1\frac{\partial^2\phi}{\partial\xi_2^2}\right) - \left(\frac{\partial^2\phi}{\partial\xi_2^2}\frac{\partial^2 w}{\partial\xi_1^2}\right. \qquad (1.19)$$

$$\left. - 2\frac{\partial^2\phi}{\partial\xi_1\partial\xi_2}\frac{\partial^2 w}{\partial\xi_1\partial\xi_2} + \frac{\partial^2\phi}{\partial\xi_1^2}\frac{\partial^2 w}{\partial\xi_2^2}\right) - P_N = 0$$

1.3.5 Specialization to the Doubly-Curved Shallow Shells Referred to Cartesian Coordinate System

As the shell is shallow, the radii of curvature are constant and Lame's parameters are equal to unity. The middle surface of a doubly-curvedshell is defined by

$$Z = \frac{X^2}{2p_1} + \frac{Y^2}{2p_2} \tag{1.20}$$

$p_1 = R_X$
$p_2 = R_Y$ for elliptic paraboloid

$p_1 = -R_X$
$p_2 = R_Y$ for hyperbolic paraboloid

$p_1 = R$
$p_2 = R$ for spherical shell

1.3.6 Strain-Displacement Relations

$$\varepsilon_X = \frac{\partial u}{\partial X} + \frac{w}{R_X} + \tfrac{1}{2}\left(\frac{\partial w}{\partial X}\right)^2$$

$$\varepsilon_Y = \frac{\partial v}{\partial Y} + \frac{w}{R_Y} + \tfrac{1}{2}\left(\frac{\partial w}{\partial Y}\right)^2$$

$$2\varepsilon_{XY} = \frac{\partial u}{\partial Y} + \frac{\partial v}{\partial X} + \frac{\partial w}{\partial X}\frac{\partial w}{\partial Y} \tag{1.21}$$

$$\chi_X = -\frac{\partial^2 w}{\partial X^2}$$

$$\chi_Y = -\frac{\partial^2 w}{\partial Y^2}$$

$$\tau = \chi_{XY} + \chi_{YX} = -2\frac{\partial^2 w}{\partial X \partial Y}$$

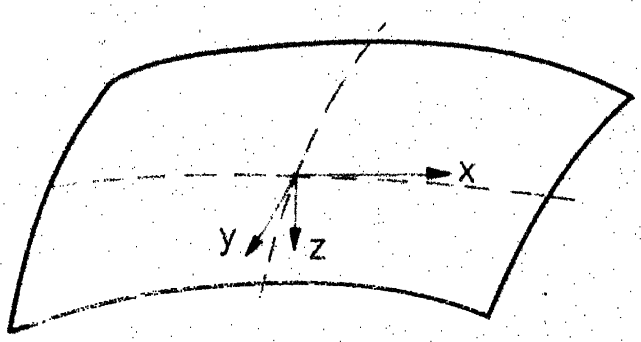

FIG. 1.3 A DOUBLY CURVED SHELL (THE EQUATION OF MIDDLE SURFACE IS $Z = x^2/2p_x + y^2/2p_y$)

1.3.7 Equilibrium Equations

$$\frac{\partial N_X}{\partial X} + \frac{\partial N_{XY}}{\partial Y} = 0$$

$$\frac{\partial N_{XY}}{\partial X} + \frac{\partial N_Y}{\partial Y} = 0$$

$$\frac{\partial M_X}{\partial X^2} + 2\frac{\partial^2 M_{XY}}{\partial X \partial Y} + \frac{\partial^2 M_Y}{\partial Y^2}$$

$$+ \frac{\partial}{\partial X}\left(N_X \frac{\partial w}{\partial X}\right) + \frac{\partial}{\partial Y}\left(N_Y \frac{\partial w}{\partial Y}\right)$$

$$+ \frac{\partial}{\partial X}\left(N_{XY} \frac{\partial w}{\partial Y}\right) + \frac{\partial}{\partial Y}\left(N_{XY} \frac{\partial w}{\partial X}\right)$$

$$- \alpha_1 \alpha_2 \left(\frac{N_X}{R_X} + \frac{N_Y}{R_Y}\right) + \alpha_1 \alpha_2 P_N = 0 \qquad (1.22)$$

Force-displacement relations are of standard form and hence are not repeated here.

1.3.8 Reduction to Two Nonlinear Equations in ϕ-w

A force function ϕ is introduced so that it satisfies the first two equilibrium equations of (1.22)

$$N_X = \frac{\partial^2 \phi}{\partial Y^2}$$

$$N_Y = \frac{\partial^2 \phi}{\partial X^2} \qquad (1.23)$$

$$N_{XY} = -\frac{\partial^2 \phi}{\partial X \partial Y}$$

The equations can be reduced to a set of two nonlinear equations in ϕ and w.

$$\nabla^2 \phi - Eh\left[\left(\frac{\partial^2 w}{\partial X \partial Y}\right)^2 - \frac{\partial^2 w}{\partial X^2}\frac{\partial^2 w}{\partial Y^2} + \frac{1}{R_X}\frac{\partial^2 w}{\partial Y^2} + \frac{1}{R_Y}\frac{\partial^2 w}{\partial X^2}\right] = 0$$

$$D\nabla^4 w + N_X\left(\frac{1}{R_X} - \frac{\partial^2 w}{\partial X^2}\right) + N_Y\left(\frac{1}{R_Y} - \frac{\partial^2 w}{\partial Y^2}\right) \qquad (1.24)$$

$$- 2N_{XY}\frac{\partial^2 w}{\partial X\, \partial Y} - P_N = 0$$

1.3.9 Single Nonlinear Differential Equation in w for the Case of General Loading

When the coordinate lines are along the principal curvatures, the differential equation becomes

$$\begin{aligned}\frac{D}{Et}\nabla^8 w = {} & \frac{\partial^2}{\partial Y^2}\left[\left\{ \left(\frac{\partial^2 w}{\partial X \partial Y}\right)^2 - \frac{\partial^2 w}{\partial X^2}\frac{\partial^2 w}{\partial Y^2} - k_1\frac{\partial^2 w}{\partial Y^2} - k_2\frac{\partial^2 w}{\partial X^2}\right\}\right. \\ & \left.(k_1 + \nabla^4\frac{\partial^2 w}{\partial X^2})\right] + \frac{\partial^2}{\partial X^2}\left[\left\{ \left(\frac{\partial^2 w}{\partial X \partial Y}\right)^2 - \frac{\partial^2 w}{\partial X^2}\frac{\partial^2 w}{\partial Y^2}\right.\right. \\ & \left.\left. - k_1\frac{\partial^2 w}{\partial Y^2} - k_2\frac{\partial^2 w}{\partial X^2}\right\}(k_2 + \nabla^4\frac{\partial^2 w}{\partial Y^2})\right] \\ & - 2\frac{\partial^2}{\partial X \partial Y}\left[\left(\frac{\partial^2 w}{\partial X \partial Y}\right)^2 - \frac{\partial^2 w}{\partial X^2}\frac{\partial^2 w}{\partial Y^2} - k_1\frac{\partial^2 w}{\partial Y^2} - K_2\frac{\partial^2 w}{\partial X^2}\right] \\ & - \frac{1}{E_t}\nabla^4\left(P_X\frac{\partial w}{\partial X} + P_Y\frac{\partial w}{\partial Y} - P_N\right)\end{aligned} \qquad (1.25)$$

1.3.10 u-v-w Formulation of the Differential Equations

When the coordinates are along the principal curvatures,

$$\frac{\partial^2 u}{\partial X^2} + \frac{1-\nu}{2}\frac{\partial^2 u}{\partial Y^2} + \frac{1+\nu}{2}\frac{\partial^2 v}{\partial X\,\partial Y} - (k_1 + \nu k_2)\frac{\partial w}{\partial X}$$

$$+ \frac{1}{2}\frac{\partial}{\partial X}\left[\left(\frac{\partial w}{\partial X}\right)^2 + \nu\left(\frac{\partial w}{\partial Y}\right)^2\right] + \frac{1-\nu}{2}\frac{\partial}{\partial Y}\left(\frac{\partial w}{\partial X}\frac{\partial w}{\partial Y}\right) = \frac{1-\nu^2}{Et}P_X$$

$$\frac{\partial^2 v}{\partial Y^2} + \frac{1-\nu}{2}\frac{\partial^2 v}{\partial X^2} + \frac{1+\nu}{2}\frac{\partial^2 u}{\partial X \partial Y} - (k_2 + \nu k_1)\frac{\partial w}{\partial Y} \qquad (1.26)$$

$$+ \frac{1}{2}\frac{\partial}{\partial Y}\left[\left(\frac{\partial w}{Y^2}\right) + \nu\left(\frac{\partial w}{\partial X}\right)^2\right] + \frac{1-\nu}{2}\frac{\partial}{\partial X}\left(\frac{\partial w}{\partial X}\frac{\partial w}{\partial Y}\right) = \frac{1-\nu^2}{Et}P_Y$$

$$- (k_1 + \nu k_2)\frac{\partial u}{\partial X} + (k_2 + \nu k_1)\frac{\partial v}{\partial Y} + (k_1^2 + k_2^2 + 2\nu k_1 k_2)w$$

$$+ \frac{t^2}{12}\left[\nabla^2\nabla^2 w + (k_1^2 + \nu k_2^2)\frac{\partial^2 w}{\partial X^2} + (k_2^2 + \nu k_1^2)\frac{\partial^2 w}{\partial Y^2}\right]$$

$$- \frac{k_1}{2}\left[\left(\frac{\partial w}{\partial X}\right)^2 + \nu\left(\frac{\partial w}{\partial Y}\right)^2\right] - \frac{k_2}{2}\left[\left(\frac{\partial^2 w}{\partial Y}\right)^2 + \nu\left(\frac{\partial w}{\partial X}\right)^2\right]$$

$$= \frac{P_N}{Et}(1-\nu^2)$$

1.3.11 Elastic Edge Beam Boundary Conditions

Referring to Figure 1.4, the following boundary conditions are deduced for edge beam parallel to Y-axis

$$EI\frac{\partial^4 w}{\partial Y^4} - D\left[\frac{\partial^3 w}{\partial X^3} + (2-\nu)\frac{\partial^3 w}{\partial X \partial Y^2}\right] - p + e\frac{\partial^3 \phi}{\partial X \partial Y^2} = 0$$

$$\kappa\frac{\partial^3 w}{\partial X \partial Y^2} - e\frac{\partial^2 \phi}{\partial Y^2} - \frac{1}{2}bD\left[\frac{\partial^3 w}{\partial X^3} + (2-\nu)\frac{\partial^3 w}{\partial X \partial Y^2}\right]$$

$$+ D\left(\frac{\partial^2 w}{\partial X^2} + \nu\frac{\partial^2 w}{\partial Y^2}\right) = 0 \qquad (1.27)$$

$$Ei\frac{\partial^4 w}{\partial Y^4} + \frac{\partial^2 \phi}{\partial Y^2} + \frac{b}{2}\frac{\partial^3 \phi}{\partial X \partial Y^2} = 0$$

$$\frac{N}{bd} = -E\,e\frac{\partial^2 w}{\partial Y^2} + \frac{1}{t}\left(\frac{\partial^2 \phi}{\partial X^2} - \nu\frac{\partial^2 \phi}{\partial Y^2}\right)$$

$e=(d-h)/2$

I_x, I_y Second moments of area of the beam cross section about major and minor axes respectvely

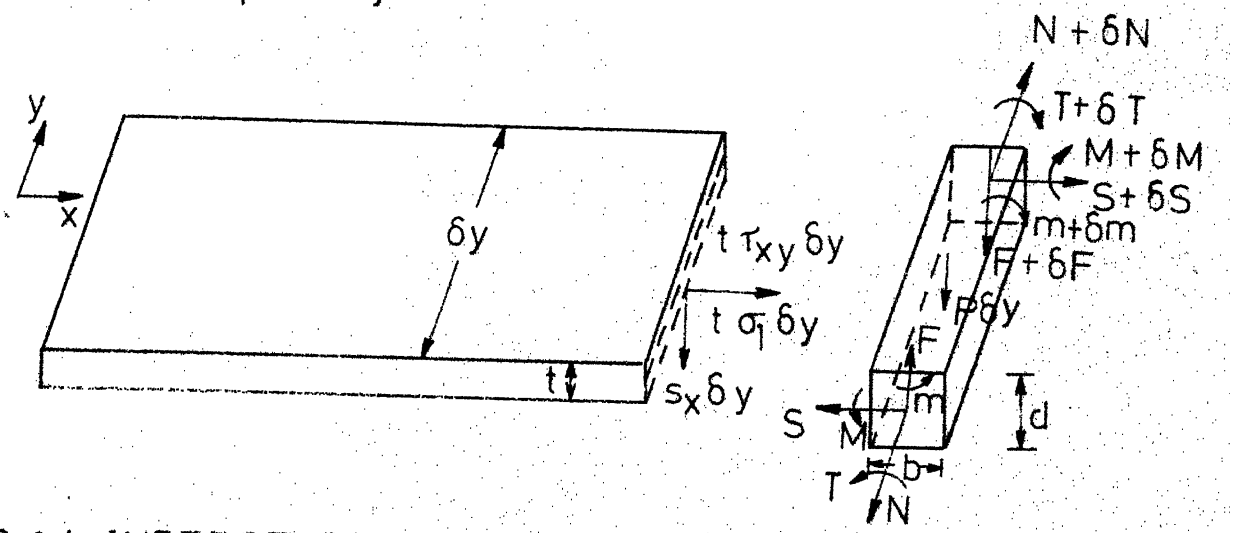

FIG. 1·4 INTERSECTION OF SHELL SURFACE WITH EDGE BEAM PARALLEL TO y-AXIS

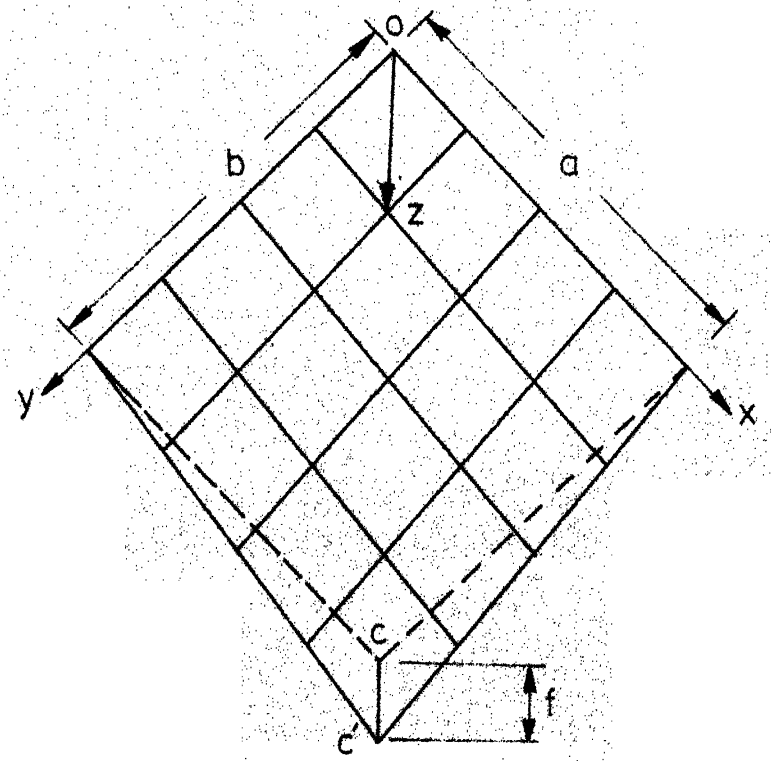

FIG 1·5 HYPERBOLIC PARABOLOID SHELL SPAN 2a AND 2b AND RISE 'f'. EQUATION OF SHELL SURFACE $z=k_1xy$ WHERE $k_1=f/ab$

1.3.12 Nonlinear Differential Equations Specialized with respect to Hyperbolic Paraboloid Shell Bounded by Characteristics

From Figure 1.5, the equation for the shell middle surface is given $Z = \frac{f}{ab} XY$. Equations (1.24) become (58)

$$\frac{1}{Et} \nabla^4 \phi - \{ \left(\frac{\partial^2 w}{\partial X \partial Y}\right)^2 - \frac{\partial^2 w}{\partial X^2} \frac{\partial^2 w}{\partial Y^2} + 2k_1 \frac{\partial^2 w}{\partial X \partial Y} = 0$$

$$D \nabla^4 w + 2k_1 \frac{\partial^2 \phi}{\partial X \partial Y} - \left(\frac{\partial^2 w}{\partial Y^2} \frac{\partial^2 w}{\partial X^2} - 2 \frac{\partial^2 \phi}{\partial X \partial Y} \frac{\partial^2 w}{\partial X \partial Y}\right. \tag{1.28}$$

$$\left. + \frac{\partial^2 \phi}{\partial X^2} \frac{\partial^2 w}{\partial Y^2}\right) - P_N = 0$$

where $k_1 = \frac{f}{ab}$

1.4 OBJECT AND SCOPE

The objective of this study is to apply the finite element method to the bending analysis of thin shallow hyperbolic paraboloid shells bounded by characteristics to a wide variety of boundary conditions including skew ones. Doubly-curved rectangular elements of negative Gaussian curvature with five degrees of freedom at each node have been used in the analysis. The analysis has been extended to the study of geometrically nonlinear behaviour of the above shell with fixed edges. The same may be applied to hyperbolic paraboloid shells with elastic edge beams. Attention has been confined to static analysis only assuming a homogeneous and isotropic shell material.

Normally, torsional rigidity (9) and the inplane bending stiffness of edge beams (12) are neglected as well as their eccentricity, if any, with respect to the shell middle surface. Inclusion of these factors presents no difficulty in the present analysis.

The whole stiffness matrix is generated by numerical integration method using six point Gauss-Legendre quadrature since the stiffness matrix for the nonlinear case also is to be evaluated numerically. Attempt is also made to use the stiffness for shallow doubly-curved shell as developed by Connor and Brebbia (24) and also by Schnobrich and Pecknold (26) to verify the results. Since there weresome errors in the stiffnesses as seen from the computer results, the attempt is dropped finally as any corrective measure involves the derivation of the entire stiffness matrix which takes lot of time.

The important step in the finite element method is the selection of appropriate displacement function. The two important displacement functions being used in plate bending analysis are discussed and the twelve-parameter polynomial expression for w used by Melosh (20), Zienkiewicz (19) and many others in plate bending analysis has been adapted here.

A variety of numerical examples is presented. In order to establish the validity of the method, comparisons are made with analytical solutions for hyperbolic paraboloids bounded by characteristics, both simply-supported and fixed along the edges. Limited comparisons are made with other numerical results to further substantiate the reliability of the analysis. The dimensions of the earlier examples are retained for comparison of results.

The programming part of the problem assumes primary importance. It can be easily modified to suit dynamic and stability analyses.

CHAPTER 2

FINITE ELEMENT METHOD FORMULATION FOR LARGE DEFLECTION ANALYSIS

2.1 GENERAL

The idealization of a continuum as an assemblage of individual pieces or elements has often been used as a device for obtaining approximate solutions to problems which are insoluble in their original form (59). This discretization of the structure results in the replacement of the original governing ordinary or partial differential equations by a set of linear algebraic equations. With the general availability of high-speed electronic computers, this reduction of the problem is significant, since the solution of large systems of linear algebraic equations poses no difficulty. When two or three idimensional elements are employed, the method is generally referred to as the 'finite-element' method.

The finite element method historically has been visualized by supposing the structure to be 'cut up' or divided into a number of sub-regions or elements, which are interconnected at a finite number of points, or 'nodes'. The force-deformation properties for an individual element, expressing relationships between nodal forces and the displacements are established usually by employing a variational principle. Once this relationship is established, the remainder of the analysis follows the usual

procedure of the stiffness method of structural analysis. Thus the dtermination of the nodal force-deformation relations for the element, or 'element stiffness matrix' which is the significant portion of the analysis.

If the displacements of the structure are regarded as the fundamental unknown quantities, the principle of minimum total potential energy may be employed to obtain the element stiffness matrix. Other variational principles can be employed in the finite element method (60,20,61), however the potential energy principle is most often used (20,19) and is used here.

In any numerical approach to a given problem convergence is very important. This problem of convergence in the case of the finite element method was investigated (20,60,61). Commendable work has been done by Oliveira (62) and Fried (63). Most of the early investigations of convergence simply involved successive refinements of grid size and comparisons with existing analytical solutions. While this procedure certainly does not prove convergence, it at least allows one to gain some confidence in the method in the absence of theoretical assurances of convergence.

Melosh (20) formulated the finite element method in terms of the principle of minimum potential energy, and set forth some criteria for selecting displacement fields. He distinguished between three types of errors which can occur:

A) Idealization errors, such as those involved in replacing a shell structure by an assemblage of flat elements.

B) Discretization errors, such as those involved in assuming the form of the displacements within an element.

C) Manipulation or round-off errors in the arithmetical operations.

Variational principles can, at best, guarantee the convergence of the discretization error to zero as the grid size is refined. Thus, in order to relate the finite element method directly to variational methods, the idealization error should be minimized, if possible. The use of curved elements achieves this end in the present case.

The admissibility criterion of the coordinate functions in the conventional Rayleigh-Ritz method is equivalent to the criterion of 'sufficient' continuity*of the assumed displacements, together with the imposition of the forced boundary conditions at a later stage in the analysis. Likewise, the usual 'completeness' criterion of the Rayleigh-Ritz method is analogous to the inclusion of the rigid body displacements and constant strain states in the assumed displacements. Melosh (20) and Bazely et al (61) have enunciated these requirements. It must be clearly

---

* 'Sufficient' continuity here means that $u,v,w,w_{,x}$, and $w_{,y}$ are continuous over the entire structure.

understood that the above conditions guarantee monotonic convergence only to the true value of the potential energy. Uniform convergence to the true displacements and derivatives of displacements (i.e. stresses) does not necessarily follow. Negligence of terms representing a constant strain state has apparently resulted in convergence to incorrect results in applications to plate bending problems (63).

Bazely et al (61) have presented the argument that the only necessary requirements for convergence to the true energy level are the inclusion of a complete rigid body motion and all constant strain states, although convergence is no longer monotonic in this case. The conclusion that these requirements are sufficient to guarantee convergence is reasonable since successive refinements of grid size lead to ever increasing satisfaction of continuity between elements, thus producing, in the limit, an admissible displacement field. In support of this argument, results of plate-bending analysis comparing 'conforming' and 'non-conforming' displacement assumptions were present (61) and showed, in almost all cases and for all grid sizes, that the so-called 'non-conforming' displacement field produced superior, although not monotonically converging, results. Before proceeding further some definitions are stated below for clear understanding.

Definition 1: Displacement models, displacement functions, displacement fields, or displacement patterns are the simple functions which are assumed to approximate the displacements for each element.

Definition 2:

$$w(X) = \alpha_1 + \alpha_2 X + \alpha_3 X^2 + \ldots + \alpha_{n+1} X^{n+1} \quad (2.1)$$

Generalized coordinates or generalized displacement amplitudes are the α's, the coefficients of the polynomial in equation (2.1). The number of terms retained in the polynomial determinss the shape of the displacement model, whereas the magnitudes of the generalized coordinates govern the amplitude. These amplitudes are called 'generalized' because they are not necessarily identified with the physical displacements of the element on a one-to-one basis; rather, they are linear combinations of some of the nodal displacements and perhaps of some of the derivatives of displacements at the nodes as well. The generalized coordinates represent the minimum number of parameters necessary to specify the polynomial amplitude.

Definition 3:

$$u = \alpha_1 + \alpha_2 X + \alpha_3 Y + \alpha_4 X^2 + \alpha_5 X Y + \alpha_6 Y^2 \quad (2.2)$$

The displacement model in equation (2.2) is expressed in terms of generalized coordinates, α, and is referred to as Generalized coordinate displacement model.

Definition 4: Conforming or compatible elements are those in which the displacement models are continuous within the elements and the displacements are compatible between adjacent elements. The compatibility condition implies that the adjacent elements must deform without causing openings, overlaps, or discontinuities between the elements.

Definition 5: Complete elements are those in which the displacement models include both the rigid body displacements of the element and the constant strain states of the element.

Definition 6: Geometric isotropy, spatial isotropy, or geometric invariance is that the displacement pattern should be independent of the orientation of the local coordinate system.

Definition 7: The degrees of freedom of the element are the nodal displacements, rotations, and/or strains necessary to specify completely the deformation of the finite element. The degrees of freedom differ from the generalized coordinates in that each is specifically identified with a single nodal point and represents a displacement (or rotation or strain) having a clear physical interpretation.

Definition 8: The minimum number of degrees of freedom (or generalized coordinates) necessary for a given element is determined by the completeness requirements for convergence, the requirements of geometric isotropy and the necessity of an adequate representation of the terms in the potential

energy functional. Additional degrees of freedom beyond the minimum number may be included for any element by adding secondary external nodes or specifying as degrees of freedom higher order derivatives of displacements at the primary nodes. The latter approach is preferred because it leads to a more compact numerical formulation in the assembly process. Elements with additional degrees of freedom are called higher order elements.

Definition 9: A natural coordinate system is a local system which permits the specification of a point within the element by a set of dimensionless numbers whose magnitudes never exceed unity. Moreover, these systems usually are arranged so that some of the natural coordinates have unit magnitude at primary external nodal points. Not only does such a coordinate system generalize and simplify the formulation but also facilitates numerical integration which is required to obtain element stiffness in linear case and tangential stiffness matrix in nonlinear (geometric) analysis.

Definition 10: An interpolation function, also known as a shape function, is a function which has unit value at one nodal point, and zero value at all other nodal points.

Definition 11: Isoparametric elements are those in which the geometry and displacements of the element are described in terms of the same parameters and are of the same order.

Definition 12: It is not necessary that the geometry and displacements of an element be expressed by the same order model. Subparametric elements are those elements for which the geometry is determined by a lower order model than the displacements. Elements for which the converse is true are called superparametric elements.

There are two types of boundary conditions, geometric boundary conditions or forced boundary conditions and natural or free boundary conditions. Geometric boundary conditions can be further categorized as being homogeneous or nonhomogeneous and as normal or skewed.

In practice, it may be true that neither inter-element continuity nor inclusion of a complete rigid body displacement is all important, as Haisler and Stricklin (64) have shown that omission of rigid body terms for shells of revolution does not affect convergence. This conclusion is borne out by results, not reported herein, of comparative studies using element stiffness matrices derived subsequently with and without inclusion of complete rigid body motions. A choice arises between achieving inter-element continuity and including a complete rigid body displacement. One of the examples will show later on the results obtained choosing the latter. When the finite element method is regarded as a physical idealisation ratherthan a mathematical one, it is better to deal with a stiffness matrix which is

'equilibrated' that is, one which gives rise to self-equilibrating nodal forces due to nodal displacements, and this is achieved through the inclusion of a complete rigid body motion in the assumed displacements. In principle it is possible to include Lagrangian multiplier terms to take into account the effect of discontinuities (64). However, this significantly increases the computational effort involved in obtaining a solution. It seems preferable instead to refine the grid size in order to obtain greater accuracy.

2.2 GEOMETRICAL RELATIONS

ξ_1, ξ_2 represent a set of orthogonal curvilinear coordinates for the middle surface and ζ the normal coordinate. The differential arc lengths along the parametric lines are denoted by dS_j ($j = 1,2$) and the differential surface area by dA. $\bar{t}_1$, $\bar{t}_2$, $\bar{n}$ define unit vectors pointing in the ξ_1, ξ_2 and ζ directions. Referring to Figure 2.1, the geometrical relations are

$$dS_j = \alpha_j \, d\xi_j$$

$$\alpha_j = \left| \frac{\bar{r}}{j} \right| = |\bar{r}, j|$$

$$\bar{t}_j = \frac{1}{\alpha_j} \bar{r}, j$$

$$\bar{n} = \bar{t}_1 \times \bar{t}_2$$

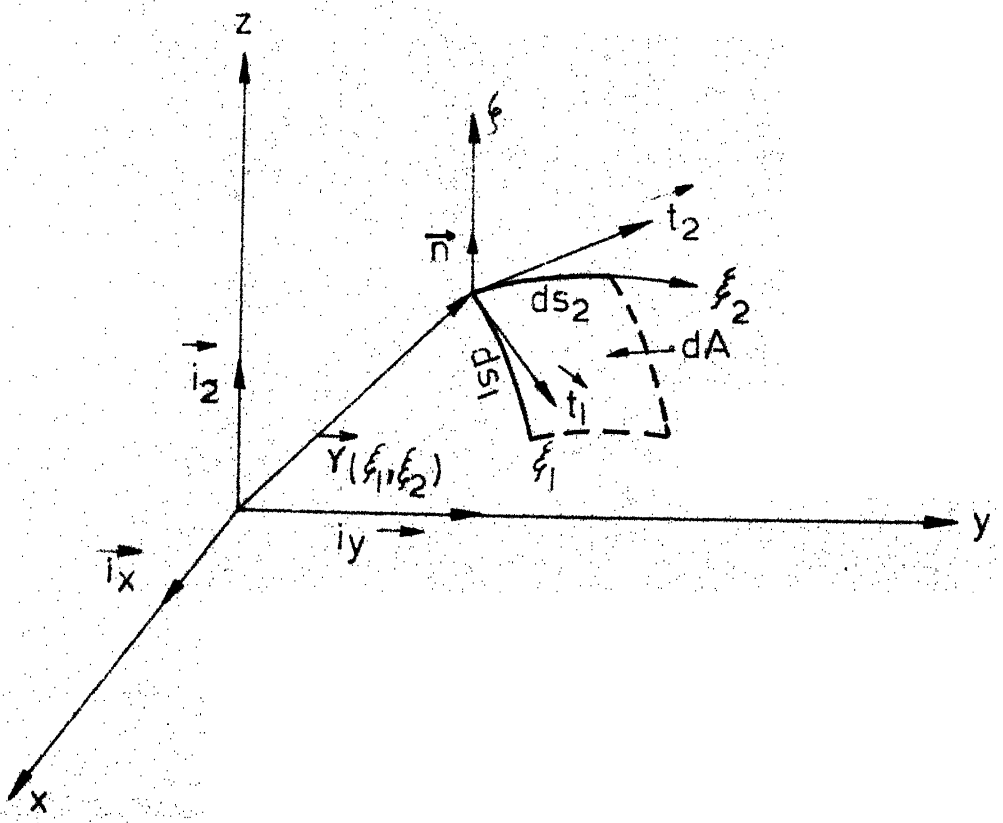

FIG. 2·1 GEOMETRICAL NOTATION
(Middle surface)

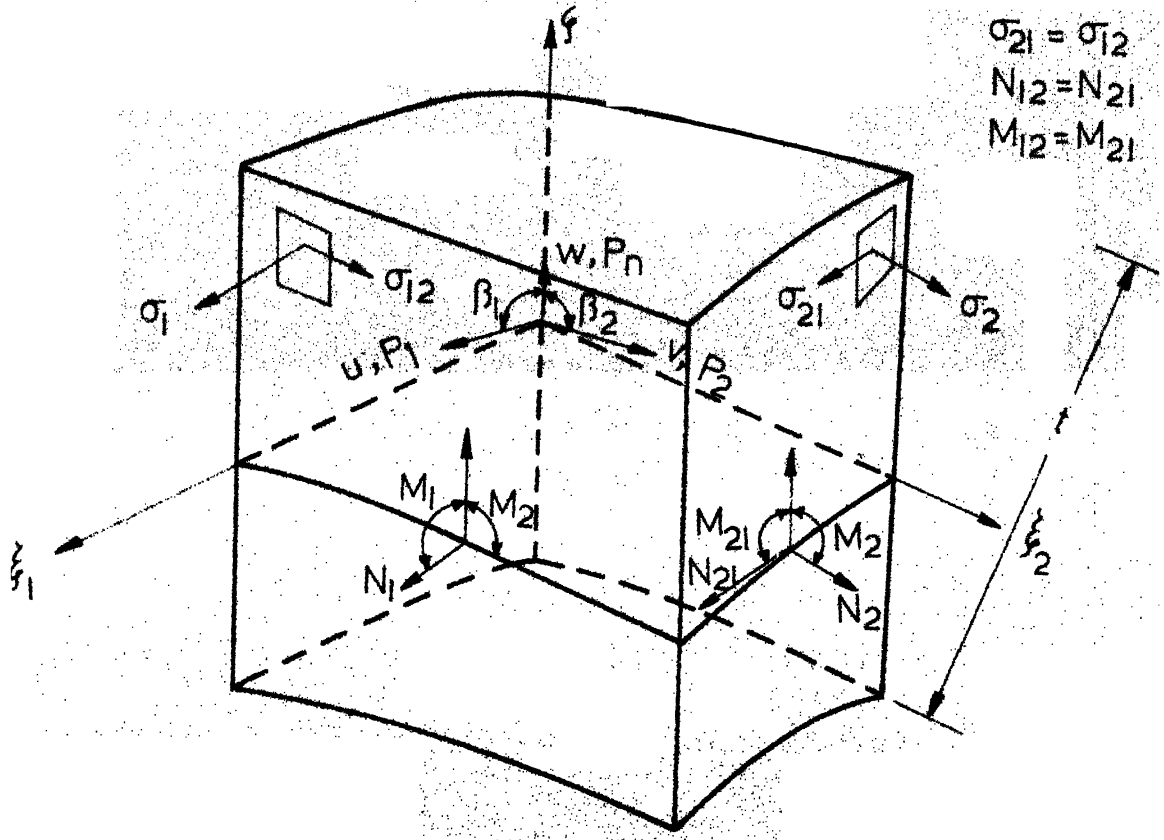

FIG. 2·2 NOTATION FOR STRESS AND DISPLACEMENTS

$$dA = dS_1\, dS_2$$

$$\frac{1}{R_{ij}} = -\frac{1}{\alpha_i\, \alpha_j}\, \bar{n}\, \bar{r}_{,ij} \qquad (i,j = 1,2) \tag{2.3}$$

in which $\bar{r}$ = the position vector to a point on the middle surface,

α_j = the surface metrics

and $\frac{1}{R_{ij}}$ = the curvatures.

For the cartesian case, ξ_1 becomes X and ξ_2 becomes Y. The surface, Z = Z(X, Y), is said to be shallow when

$$Z,_X{}^2 << 1 \; ; \quad Z,_Y{}^2 << 1 \tag{2.2}$$

Specializing (66) for the shallow case leads to

$$\alpha_1 \simeq \alpha_2 \simeq 1$$

$$\bar{t}_1 = \bar{i}_X + Z,_X\, \bar{i}_Z$$

$$\bar{t}_2 = \bar{i}_Y + Z,_Y\, \bar{i}_Z$$

$$\bar{n} = -Z,_X\, \bar{i}_X - Z,_Y\, \bar{i}_Y + \bar{i}_Z \tag{2.4}$$

$$\frac{1}{R_{11}} = -Z,_{XX}$$

$$\frac{1}{R_{22}} = -Z,_{YY}$$

$$\frac{1}{R_{12}} = -Z,_{XY}$$

2.3 DEFORMATION-DISPLACEMENT RELATIONS

Referring to the Figure 2.2, the strain matrix $[\varepsilon]$ at (Ξ_1, Ξ_2, ζ) is expressed as

$$[\varepsilon] = \{ \varepsilon_1, \varepsilon_2, \varepsilon_{12} \}_{\xi_1, \xi_2, \zeta} \tag{2.5}$$

in which ε_1, ε_2 = extensional strains (ξ_1, ξ_2 directions); and ε_{12} = the shear strain. Considering the shell to be thin and neglecting transverse shear deformation, the strain varies linearly over the thickness and can be expressed as

$$[\varepsilon] = [e] + \zeta\, [k] \tag{2.6}$$

in which [e] contains the stretching deformations and [k] contains the curvature changes for the middle surface.

The expressions for [e] and [k] used in this study are

$$[e] = [e]_\ell + [e]_r$$

$$[e]_\ell = \begin{Bmatrix} u_{1,X} - Z_{,XX}\, w \\ u_{2,Y} - Z_{,YY}\, w \\ u_{1,Y} + u_{2,X} - 2\, Z_{,XY}\, w \end{Bmatrix}$$

$$[e]_r = \tfrac{1}{2} \begin{Bmatrix} w_{,X}^2 \\ w_{,Y}^2 \\ 2 w_{,X}\, w_{,Y} \end{Bmatrix} \tag{2.7}$$

$$[k] = - \begin{Bmatrix} w,_{XX} \\ w,_{YY} \\ 2w,_{XY} \end{Bmatrix}$$

$$\beta_1 = -w,_X$$

$$\beta_2 = -w,_Y$$

These relations are restricted to small rotations, i.e. $\beta_i^2 << 1$.

2.4 FORCE-DEFORMATION RELATIONS, STRAIN ENERGY DENSITY

Stress matrix $[\sigma]$ corresponding to $[\varepsilon]$ is expressed as

$$[\sigma] = \{\sigma_1, \ \sigma_2, \ \sigma_{12}\} \tag{2.8}$$

and express the stress-strain relations as

$$[\sigma] = [D] \ ([\varepsilon] - [\varepsilon]^0) \tag{2.8a}$$

in which $[\varepsilon]^0$ contains the initial strains. It is assumed that initial strains also vary linearly over the thickness, 't', and write

$$[\varepsilon]^0 = [e]^0 + \zeta [k]^0 \tag{2.9}$$

in which

$$[e]^0 = \frac{1}{t} \int [\varepsilon]^0 \, d\zeta$$

$$[k]^0 = \frac{12}{t^3} \int \zeta [\varepsilon]^0 \, d\zeta \tag{2.10a}$$

The expressions for the stress resultants and stress couples follow from the definition, expressed as

$$[N] = \int [\sigma]\, d\zeta = \{ N_1, N_2, N_{12}\}$$
$$[M] = \int \zeta\, [\sigma]\, d\zeta = \{ M_1, M_2, M_{12}\} \qquad (2.10b)$$

and are written as

$$[N] = [N]^0 + [D]_S([e]_\ell + [e]_r)$$
$$[M] = [M]^0 + [D]_b\, [k] \qquad (2.11)$$

in which

$$[N]^0 = -[D]_S\, [e]^0$$

and (2.12)

$$[M]^0 = -[D]_b\, [k]^0$$

$$[D]_S = t[D] = \text{Stretching rigidity matrix}$$
$$[D]_b = \frac{t^3}{12}[D] = \text{Bending rigidity matrix} \qquad (2.13)$$

V represents the strain energy per unit area of the middle surface. By definition, the first variation is given by

$$\delta V = \int [\sigma]^T\, \delta[\varepsilon]\, d\zeta = [N]^T\, \delta[e] + [M]^T\, \delta[e] \qquad (2.14a)$$

The second variation is obtained by operating on δV, expressed as

$$\delta^2 V = \delta(\delta V)$$
$$= [N]^T\, \delta^2[e] + \delta[N]^T\, \delta[e] + [M]^T\, \delta^2[k] + \delta[M]^T\, \delta[k] \qquad (2.14b)$$

As $[e]_{\ell}$ and $[k]$ are linear functions

$$\delta^2[e]_{\ell} = \delta^2[k] = [0]$$
$$\delta^2[e] = \delta^2[e]_r \qquad (2.14c)$$

Substituting for $[N]$ and $[M]$ using equations (2.11) and noting that $[N]^0$ and $[M]^0$ are constant,

$$\delta V = (\delta[e]_{\ell} + \delta[e]_r)^T [[N]^0 + [D]_S ([e]_{\ell} + [e]_r)] + (\delta[k])^T ([M]^0 + [D]_b [k]) \qquad (2.15)$$

$$\delta^2 V = (\delta^2[e]_r)^T [N] + (\delta[e]_{\ell} + \delta[e]_r)^T [D]_S (\delta[e]_{\ell} + \delta[e]_r) + (\delta[k])^T [D]_b \delta[k] \qquad (2.16)$$

2.5 ELEMENT STIFFNESS AND NODAL FORCE MATRICES

$[u]$ and $[p]$ define the middle surface translation and external force intensity matrices referred to the initial local reference frame as shown in Figure 2.2, expressed as

$$[u] = \{ u_1, u_2, w\}$$
$$[p] = \{ p_1, p_2, p_n\} \qquad (2.17)$$

The governing equilibrium equations are obtained by applying the principle of virtual displacements which requires

$$\int \delta V \, d\, A = \int [p]^T \delta[u] \, d\, A \qquad (2.18)$$

to be satisfied for arbitrary permissible $\delta[u]$. Also, the consistent linearized incremental equations are determined

by taking variation of equation (2.18), expressed as

$$\int \delta^2 V \, d A = \int \delta[p]^T \; \delta[u] \, d A \qquad (2.19)$$

In this section, the expansion of equation (2.18) is considered. Equation (2.19) is utilized later on in connection with the Newton-Raphson method.

The expansion of [u] over element n can be expressed as

$$[u] = [A] \, [\alpha]_n \qquad (2.20)$$

in which $[\alpha]_n$ contains the generalized coordinates for element n and [A] contains prescribed functions of the local coordinates.

Substituting for [u] in equation (2.6) leads to

$$\begin{aligned} [e]_\ell &= [B]_{S\ell} \, [\alpha]_n \\ [e]_r &= [B]_{Sr} \, [\alpha]_n \\ [k] &= [B]_b \, [\alpha]_n \end{aligned} \qquad (2.21)$$

The variations are

$$\begin{aligned} \delta[e]_\ell &= [B]_{S\ell} \, \delta[\alpha]_n \\ \delta[e]_r &= [B]^*_{Sr} \, \delta[\alpha]_n \\ \delta[k] &= [B]_b \; \delta[\alpha]_n \end{aligned} \qquad (2.22)$$

It is significant to note that $[B]_{Sr}$ and $[B]^*_{Sr}$ depend on $[\alpha]_n$ whereas $[B]_{S\ell}$ and $[B]_b$ are independent of $[\alpha]_n$. Substituting equations (2.21) and (2.22) into equation (2.15),

and integrating over the element, the result may be written as

$$\int_{\text{element } n} \delta V \, dA = \delta[\alpha]_n^T \left[[\bar{k}]_n [\alpha]_n + [\bar{p}]_n^0 \right] = \delta[\alpha]_n^T [\bar{p}]_{int,n} \tag{2.23}$$

in which

$$[\bar{K}]_n = \int_{\text{element } n} [([B]_{S\ell} + [B]_{Sr}^*)^T [D]_{S\ell} ([B]_S + [B]_{Sr}) + [B]_b^T [D]_b [B]_b] \, dA \tag{2.24a}$$

and

$$[\bar{P}]_n^0 = \int_{\text{element } n} [([B]_{S\ell} + [B]_{Sr}^*)^T [n]^0 + [B]_b^T [M]^0] dA \tag{2.24b}$$

The term involving the external loading is written as

$$\int_{\text{element } n} [p]^T \delta[u] \, dA = \delta[\alpha]_n^T [\bar{P}]_{ext,n} \tag{2.25}$$

in which

$$[\bar{P}]_{ext,n} = \int_{\text{element } n} [A]^T [p] \, dA \tag{2.26}$$

2.6 LINEAR STATIC CASE

For the case of the shell undergoing time-independent deformations, Hamilton's principle becomes the principle of minimum potential energy. If the deformations are assumed small-linear static case - $[B]_{Sr}$ and $[B]_{SR}^*$ matrices are zero. Thus, the element stiffness and force matrices are,

$$[\bar{K}]_{\ell,n} = \int_{\text{element } n} ([B]_{S\ell}^{T}[D]_{S}[B]_{S\ell} + [B]_{b}^{T}[B]_{b})dA$$

$$[\bar{P}]_{n}^{O} = \int_{\text{element } n} ([B]_{S\ell}^{T}[N]^{O} + [B]_{b}^{T}[M]^{O}\, dA \qquad (2.27)$$

$$[\bar{P}]_{ext,n} = \int_{\text{element } n} [A]^{T}[p]\, dA$$

The general system of equations is,

$$[\bar{K}]_{\ell}[u] = [P] \qquad (2.28)$$

The displacement boundary conditions can be applied to the above and the resulting system of linear simultaneous equations can be solved for the nodal displacement vector [u]. Once [u] is known, the element nodal displacements $[U]_n$ for each element can be obtained. Thus using equations already shown, strains and the corresponding forces and moments can be obtained.

2.7 GEOMETRICALLY NONLINEAR STATIC CASE

This case corresponds to one of time-independent loading on the shell but with large out of plane rotations. In this case, the nonlinear terms in [e] have to be taken into account. Thus, the terms, $[B]_{Sr}$ and $[B]_{Sr}^{*}$, are due to geometrical nonlinearity. The expressions for $[e]_r$ and $\delta[e]_r$ are used to generate the matrices $[B]_{Sr}$ and $[B]_{Sr}^{*}$.

$$[e]_r = [B]_{Sr}\,[\alpha]_n = \tfrac{1}{2}\begin{Bmatrix} (w,_X)^2 \\ (w,_Y)^2 \\ 2w,_X\, w,_Y \end{Bmatrix} \qquad (2.29)$$

$$\delta[e]_r = [B]^*_{Sr}\,[\alpha]_n = \begin{Bmatrix} w,_X\ \delta w,_X \\ w,_Y\ \delta w,_Y \\ w,_X\ \delta w,_Y + w,_Y\ \delta w,_X \end{Bmatrix}$$

The form of equation (2.29a) suggests working with $\{w,_X,\ w,_Y\}$ and

$$[\omega]^* = \begin{bmatrix} w,_X & 0 \\ 0 & w,_Y \\ w,_Y & w,_X \end{bmatrix} \qquad (2.29b)$$

$$\text{Then } [e]_r = \tfrac{1}{2}\,[\omega]^* \begin{Bmatrix} w,_X \\ w,_Y \end{Bmatrix} \qquad (2.29c)$$

$$\delta[e]_r = [\omega]^* \begin{Bmatrix} \delta w,_X \\ \delta w,_Y \end{Bmatrix}$$

Continuing

$$\begin{Bmatrix} w,_X \\ w,_Y \end{Bmatrix} = [A]_r\,[\alpha]_n \qquad (2.30)$$

It follows that

$$[B]_{Sr} = \tfrac{1}{2}[B]^*_{Sr}$$
$$[B]^*_{Sr} = [\omega]^*[A]_r \qquad (2.31)$$

$[\omega]^*$ depends on $[\alpha]_n$ and the local coordinates. It is convenient to segregate the nonlinear terms in the expression for $[\bar{K}]_n$ and $[\bar{P}]_n^0$. Therefore,

$$[\bar{K}]_n = [\bar{K}]_{\ell,n} + [\bar{K}]_{r,n}$$
$$[\bar{P}]_n^0 = [\bar{P}]_{\ell,n}^0 + [\bar{P}]_{r,n}^0 \qquad (2.32)$$

in which $[\bar{K}]_{\ell,n}$, $[\bar{P}]_{\ell,n}^0$ are the linear terms, expressed as

$$[\bar{K}]_{\ell,n} = \int_{\text{element } n} ([B]_{S\ell}^T [D]_S [B]_{S\ell} + [B]_b^T [D]_b [B]_b) dA$$
$$[\bar{P}]_{\ell,n}^0 = \int_{\text{element } n} ([B]_{S\ell}^T [N]^0 + [B]_b^T [M]^0)\, dA \qquad (2.33)$$

and $[\bar{K}]_{r,n}$ and $[\bar{P}]_{r,n}^0$ depend on $[\alpha]_n$, expressed as

$$[\bar{K}]_{r,n} = \int_{\text{element } n} [\tfrac{1}{2}[B]_{S\ell}^T [D]_S [B]_{Sr}^* + ([B]_{S\ell}^T)[D]_S [B]_{Sr}^*)^T$$
$$+ \tfrac{1}{2}([B]_{Sr}^*)^T [D]_S [B]_{Sr}^*] dA \qquad (2.34)$$
$$[\bar{P}]_{r,n}^0 = \int_{\text{element } n} [([B]_{Sr}^*)^T [N]^0] dA$$

Explicit forms for the integrals can be obtained for the nonlinear matrices but the computations are difficult. Fellippa (40) and Gallagher et al (84) assume $[\omega]^*$ is constant over the element. However, it is preferred to use the exact expression for $[\omega]^*$ and evaluate the integrals numerically.

It remains to substitute for the element parameters, $[\alpha]_n$, in terms of the nodal displacements. Five degrees of freedom per node are considered, namely, middle surface translations u_1, u_2 and w, and normal rotations β_1 and β_2. The number of nodal displacement quantities depend on the expansions for polynomials used. For example, Schmit (86) worked with 12 per node. The above applied both for nonlinear flat plate analysis and for shallow shell analysis. $[U]_j$ denotes the displacement matrix for node j, expressed as

$$[U]_j = \{ u_1, u_2, w, \beta_1, \beta_2 \}_{\text{node } j} \tag{2.35}$$

$[U]_{E,n}$ represents the matrix containing the nodal displacement matrices for element listed in a prescribed order.

$$[U]_{E,n} = \{ [U]_{n_1}, [U]_{n_2}, \ldots, [U]_{n_{Sn}} \} \tag{2.36}$$

in which S_n = the total number of nodes and n_i $(i=1,2,\ldots,S_n)$ are the node numbers. Figures 2.3 shows the notation specialized for a rectangular element having nodes at the corner points.

Using equation (2.20),

$$\begin{aligned} [U]_{E,n} &= [C]_n [\alpha]_n \\ [\alpha]_n &= [C]_n^{-1} [U]_{E,n} \end{aligned} \tag{2.37}$$

Substituting for $[\alpha_n]$ in equations (2.23) and (2.25),

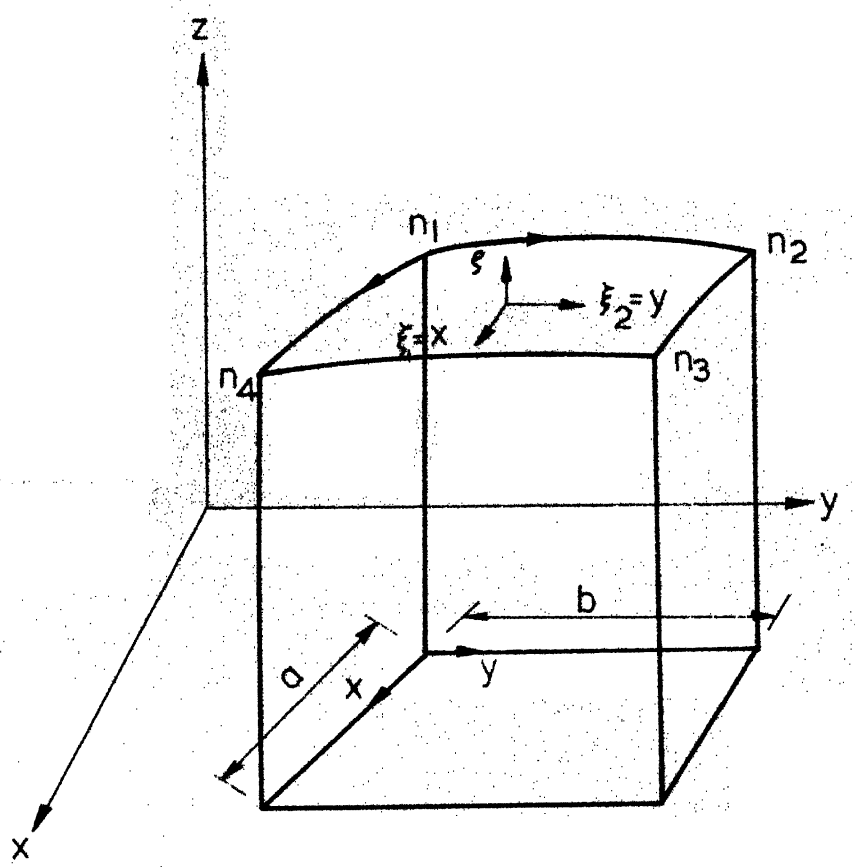

FIG. 2·3 ELEMENT NOTATION: CARTESIAN CASE

$$\int_{\text{element } n} \delta V \, dA = \delta[U]^T_{E,n}([K]_n [U]_{E,n} + [P]^0_n) = \delta[U]^T_{E,n}[P]_{int,n}$$

$$\int_{\text{element } n} [p]^T \, dA = \delta[U]^T_{E,n} [P]_{ext,n} \qquad (2.38)$$

in which

$$[K]_n = [C]_n^{-1,T} [\bar{K}]_n [C]_n^{-1}$$

$$[P]^0_n = [C]_n^{-1,T} [\bar{P}]^0_n \qquad (2.39)$$

$$[P]_{ext,n} = [C]^{-1,T} [\bar{P}]_{ext,n}$$

interpreting $[K]_n$ and $[P_n]$ as element stiffness and nodal force matrices. Finally, substituting for $[\bar{K}]_n$ and $[\bar{P}]^0_n$ using equation (2.32)

$$[K]_n = [K]_{\ell,n} + [K]_{r,n}$$
$$\text{and } [P]^0_n = [P]^0_{\ell,n} + [P]^0_{r,n} \qquad (2.40)$$

are obtained, in which the terms in $[K]$ and $[P]^0_n$ are determined by applying equation (2.37) to equations (2.31) and (2.32).

2.7.1 System Equations

$[u]$, defined as the nodal displacement matrix, is expressed as

$$[u] = \{ [U]_1, [U]_2, \ldots, [U]_{n_N} \} \qquad (2.41)$$

in which n_N represents the total number of nodes and the

summation of equation (2.38) over the elements is expressed as

$$\sum_{n=1}^{n_E} \int_{\text{element } n} \delta V \, dA = \sum_{n=1}^{n_E} \delta[U]^T_{E,n} [P]_{int,n} = \delta[u]^T[p]_{int} \tag{2.42}$$

$$\sum_{n=1}^{n_E} \int_{\text{element } n} [p]^T \delta[u] dA = \sum_{n=1}^{n_E} \delta[U]^T_{E,n}[P]_{ext,n} = \delta[u]^T[p]_{ext}$$

Applying the Principle of Virtual Displacements to equation (2.42) results in equilibrium equations

$$[\psi] = [p]_{ext} - [p]_{int} = [\psi] (|u|) = [0] \tag{2.43}$$

In this study, the external loading is considered to be independent of the displacements, i.e. take $[p]_{ext}$=constant. Term $[p]_{int}$ is a nonlinear function of [u] when the rotational terms are included.

2.7.2 Newton-Raphson Iteration

In the following it is assumed that the nodal displacement boundary conditions have been introduced.

$[u]^{(i)}$ represents the ith estimate for the solution due to a particular loading.

$$[\psi]\big|_{[u]=[u]^{(i)}} = [\psi]^{(i)}$$

$$[p]_{int}\big|_{[u]=[u]^{(i)}} = [p]^{(i)}_{int} \tag{2.44}$$

The recurrence relation for Newton-Raphson iteration is

$$-\delta[\psi]^{(i)} = [\psi]^{(i)} \tag{2.45a}$$

in which $\delta[\psi]^{(i)}$ is the first order change in $[\psi]$ due to $\delta[u]$. Equation (2.45a) becomes

$$\delta[p]_{int}^{(i)} = [p]_{ext} - [p]_{int}^{(i)} \tag{2.45b}$$

$\delta[p]_{int}^{(i)}$ can be expressed as

$$\delta[p]_{int}^{(i)} = [k]_t^{(i)}\ \delta[u]^{(i)} \tag{2.45c}$$

in which $[k]_t^{(i)}$ can be interpreted as the system tangent stiffness matrix evaluated at $[u]^{(i)}$. Finally the recurrence relation takes the form

$$[k]_t^{(i)}\ \delta[u]^{(i)} = [p]_{ext} - [p]_{int}^{(i)} \tag{2.46}$$

and $[u]^{(i+1)} = [u]^{(i)} + \delta[u]^{(i)}$

A convenient measure of $[u]$ is the Euclidean norm, N, defined by

$$N = ([u]^T\ [u])^{\frac{1}{2}} \tag{2.47}$$

The convergence criteria is

$$\frac{N^{(i+1)} - N^{(i)}}{N^{(i)}} \leq \Delta \tag{2.48}$$

in which Δ = the desired accuracy.

2.7.3 Generation of Tangent Stiffness Matrix

By definition

$$\delta[u]^T[k]_t\ \delta[u] = \sum_{n=1}^{n_E} \int_{\text{element } n} \delta^2 V\ dA \tag{2.49a}$$

From equations (2.16) and (2.22)

$$\int_{\text{element n}} \delta^2 V \, dA = \int_{\text{element n}} [(\delta^2[e]_r)^T[N]dA$$

$$+ \delta[\alpha]_n^T \{ \int_{\text{element n}} [([B]_S + [B]_{Sr})^T[D]_S([B]_S + [B]_{Sr})$$

$$+ [B]_b^T [D]_b [B]_b]dA\} \delta[\alpha]_n \qquad (2.49b)$$

To proceed further, the first term

$$(\delta^2[e]_r)^T[N] = N_1(\delta w,_X)^2 + N_2(\delta w,_Y)^2 + 2N_{12}\delta w,_X \delta w,_Y \qquad (2.49c)$$

must be expressed in a quadratic form in $\delta[\alpha]_n$. By defining $[N]^*$ as

$$[N]^* = \begin{bmatrix} N_1 & N_{12} \\ N_{12} & N_2 \end{bmatrix} \qquad (2.49d)$$

$$(\delta^2[e]_r)^T[N] = \delta[\alpha]_n^T ([A]_r^T [N]^*[A]_r) \delta[\alpha]_n \qquad (2.49e)$$

can be written. Then

$$\int_{\text{element n}} \delta^2 V \, dA = \delta[\alpha]_n^T[\bar{K}]_{t,n} \delta[\alpha]_n = \delta[U]_{E,n}^T[K]_{t,n}\delta[U]_{E,n} \qquad (2.50)$$

in which

$$[\bar{K}]_{t,n} = [\bar{K}]_{\ell,n} + [\bar{K}]_{g,n} \qquad (2.51)$$

$$K_{(),n} = [C]_n^{-1,T}[\bar{K}]_{(),n} [C]_n^{-1}$$

The linear term is given by equation (2.33). The nonlinear term, which is usually referred to as the geometric stiffness matrix, has the form

$$[\bar{K}]_{g,n} = \int_{\text{element } n} [[A]_r^T [N]^* [A]_r + [B]_{S\,\ell}^T [D]_S [B]_{Sr}^* + ([B]_{S\,\ell}^T [D]_S [B]_{Sr}^*)^T + ([B]_{Sr}^*)^T [D]_S [B]_{Sr}^*] dA \tag{2.52}$$

It may be noted that $[\bar{K}]_{g,n}$ involves the same terms as $[\bar{K}]_{r,n}$; the only additional term is $[A]_r^T [N]^* [A]_r$.

2.7.4 Linearized Incremental Procedure

$[u]$ denotes the solution for a partucular loading. An incremental loading, $\Delta[p]_{ext}$ is applied. The incremental equilibrium follows from equation (2.43), expressed as

$$\Delta[p]_{ext} = \Delta[p]_{int} \tag{2.53a}$$

To determine $\Delta[p]_{int}$,

$$\delta[u]^T \Delta[p]_{int} = \sum_{n=1}^{n_E} \int_{\text{element } n} \Delta(\delta V) d\mathcal{A} \tag{2.53b}$$

Taking $\Delta(\delta V) \simeq \delta^2 V$ results in linearized incremental equations

$$\Delta[p]_{int} \simeq \delta[p]_{int} = [K]_t \Delta[u] \tag{2.53c}$$

The incremental displacement, $\Delta[u]$, due to $\Delta[p]_{ext}$ is obtained from

$$[K]_t \Delta[u] = \Delta[p]_{ext} \tag{2.54d}$$

in which $[K]_t$ is evaluated at [u], i.e., at the equilibrium position prior to the application of the load increment.

The procedure corresponds to truncating Newton-Raphson after one cycle. As the solution is approximate, the only resort is to repeat the computation using smaller load increments in order to assess the accuracy.

CHAPTER 3

SOLUTIONS FOR SMALL DEFLECTION

3.1 GENERAL

The formulation outlined in the previous chapter is valid for an arbitrary element, i.e., arbitrary shape and displacement expansions. A simple shallow rectangular element as shown in Figure 2.1 is employed. The displacement expansions are

$$
\begin{aligned}
u &= \alpha_1 + \alpha_2 X + \alpha_3 Y + \alpha_4 XY \\
v &= \alpha_5 + \alpha_6 X + \alpha_7 Y + \alpha_8 XY \\
w &= \alpha_9 + \alpha_{10} X + \alpha_{11} Y + \alpha_{12} X^2 + \alpha_{13} XY + \alpha_{14} Y^2 \\
&\quad + \alpha_{15} X^3 + \alpha_{16} X^2 Y + \alpha_{17} XY^2 + \alpha_{18} Y^3 + \alpha_{19} X^3 y \\
&\quad + \alpha_{20}\, XY^3 .
\end{aligned}
\tag{3.1}
$$

The element is unconforming (it does not satisfy normal slope compatibility) and complete rigid body motion is not taken into account. This point has been discussed in Chapter 5. In spite of non-compatibility and ommission of complete rigid body motion, it has been shown (82,64) that results obtained are still accurate. Hence the above simple displacement expansions are chosen which still give accurate results. Linear stiffness matrix for shell element is generated using numerical integration procedure as outlined

in Appendix A, as stiffness matrix given by Brebbia (67) failed to give correct results. Further the stiffness matrix obtained by numerical integration technique is checked for its accuracy by using the technique suggested by Kabaila as given in Appendix B by writing the necessary computer program.

The above developed stiffness matrix has been used in the program of the finite element method to analyse hyperbolic paraboloid shells bounded by straight edges with different boundary conditions. Since displacement formulation is used in the finite element theory by applying the Principle of Minimum Potential Energy, only forced boundary conditions are specified in the analysis. The natural boundary conditions, together with the equilibrium equations are satisfied approximately as part of the minimization procedure. Since forced boundary conditions are specified in the analysis, it might, therefore, be expected that convergence would be superior for those problems in which all or most of the boundary conditions are of the forced type. Also, the extent to which the natural boundary conditions are satisfied for a given problem can be used as a means of assessing if convergence is satisfactory in a practical sense.

A variety of problems of hyperboloid paraboloid shells bounded by characteristics for which

analytical or other numerical solutions are available, are analysed. These problems are intended to check the computer program developed independently and to substantiate the finite element method as applied to shallow shells and to enable one to evaluate in a limited sense the convergence characteristics of the element stiffness matrix generated.

3.2 SIMPLY SUPPORTED HYPERBOLIC PARABOLOID SHELL BOUNDED BY CHARACTERISTICS UNDER UNIFORM NORMAL LOAD: COMPARISON WITH SERIES SOLUTION (7)

Figure 3.1 shows a square hyperbolic paraboloid simply supported on all edges and subjected to a uniform normal load of -50 lbs/sq.ft.

Shell Data:

$a = 180$ in. $\quad E = 3 \times 10^6$ lbs/sq.in.

$b = 180$ in. $\quad \nu = 0.16$

$c = 36$ in.

$h = 2.5$ in.

A grid of (8x8) over the entire shell is used in the analysis.

Displacement boundary conditions for an edge X = constant are:

$v = 0$

$w = 0$

$\beta_2 = 0$

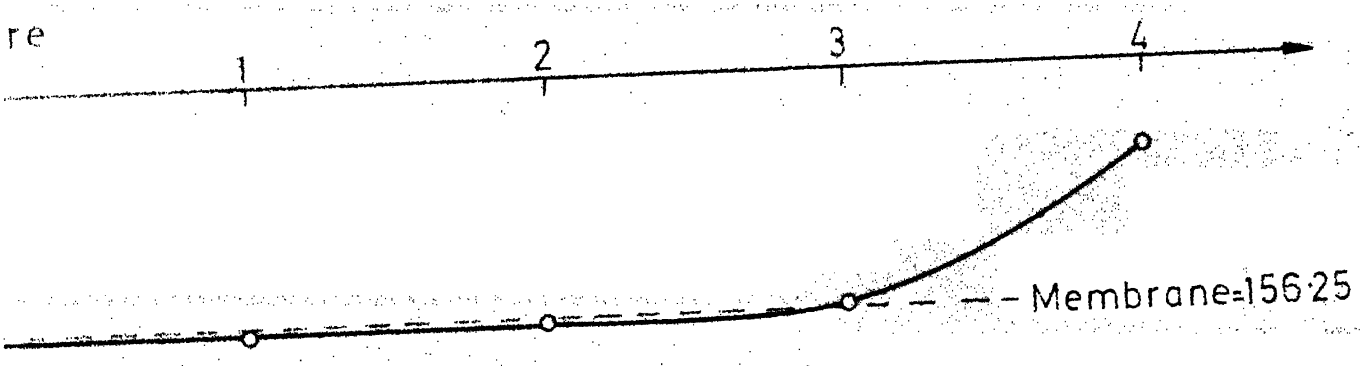

(a) Variation of N_{xy} along x axis

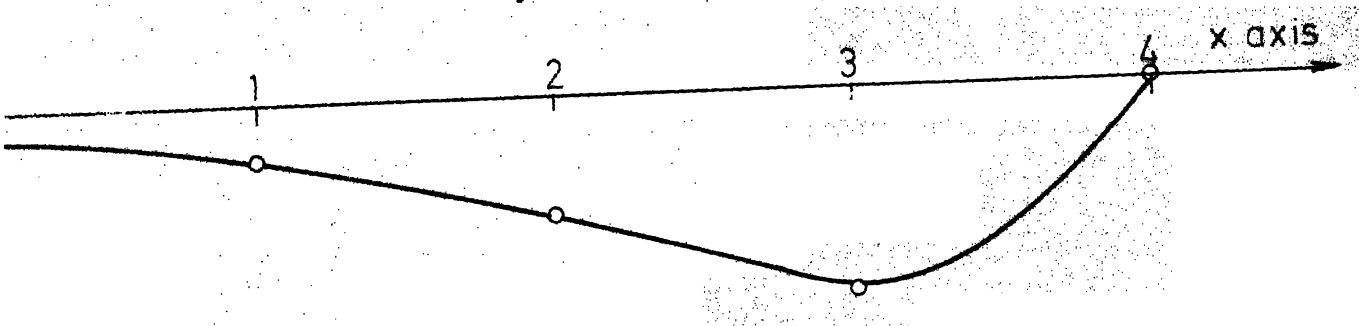

(b) Variation of M_x along x axis

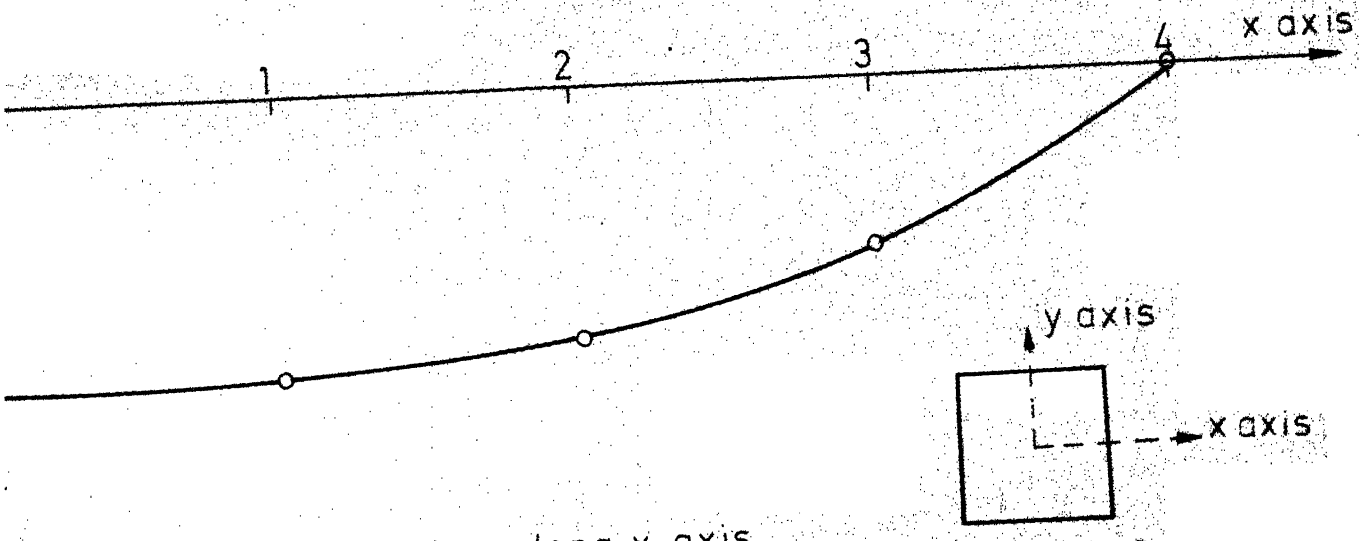

(c) Deflection along x axis

Mesh size 8×8

Data
$a = 180''$
$b = 180''$
$c = 36''$
$h = 2·5''$

$E = 3 \times 10$ lb/in^2
$\nu = 0·6$
$P_N = 50$ lb/ft^2

FIG. 3·1 HYPERBOLIC PARABOLOID SHELL WITH SIMPLY SUPPORTED EDGES UNDER UNIFORM NORMAL LOAD

Similar boundary conditions are used for an edge Y = constant. The normal deflection w, the membrane shear N_{XY} and the bending moment M_X across the section Y = 0 is plotted along X-axis from X = 0 to X = a.

All quantities plotted agree with the series solution. The membrane theory predicts a constant N_{XY} of 156.25 lbs/in. throughout the shell, while the bending theory yields a value of N_{XY} = 160 lbs/in. at the centre of the shell. The bending moment M_X is fairly large, producing bending stresses which are about half as much as the membrane stresses, and dies out slowly toward the centre of the shell.

3.3 CLAMPED HYPERBOLIC PARABOLOID BOUNDED BY CHARACTERISTICS UNDER UNIFORM NORMAL LOAD

3.3.1 Figure 3.2 shows a square hyperbolic paraboloid clamped on all edges and subjected to a uniform normal load of -1.0 lbs/sq.in. This shell has been analysed by Chetty and Tottenham (7) using a variational method.

Shell Data:

a = 6.46 in. E = 5×10^5 lbs/sq.in.

b = 6.46 in. ν = 0.39

c = 1.304 in.

h = 0.25 in.

A grid of (8x8) over the entire shell is used in the analysis.

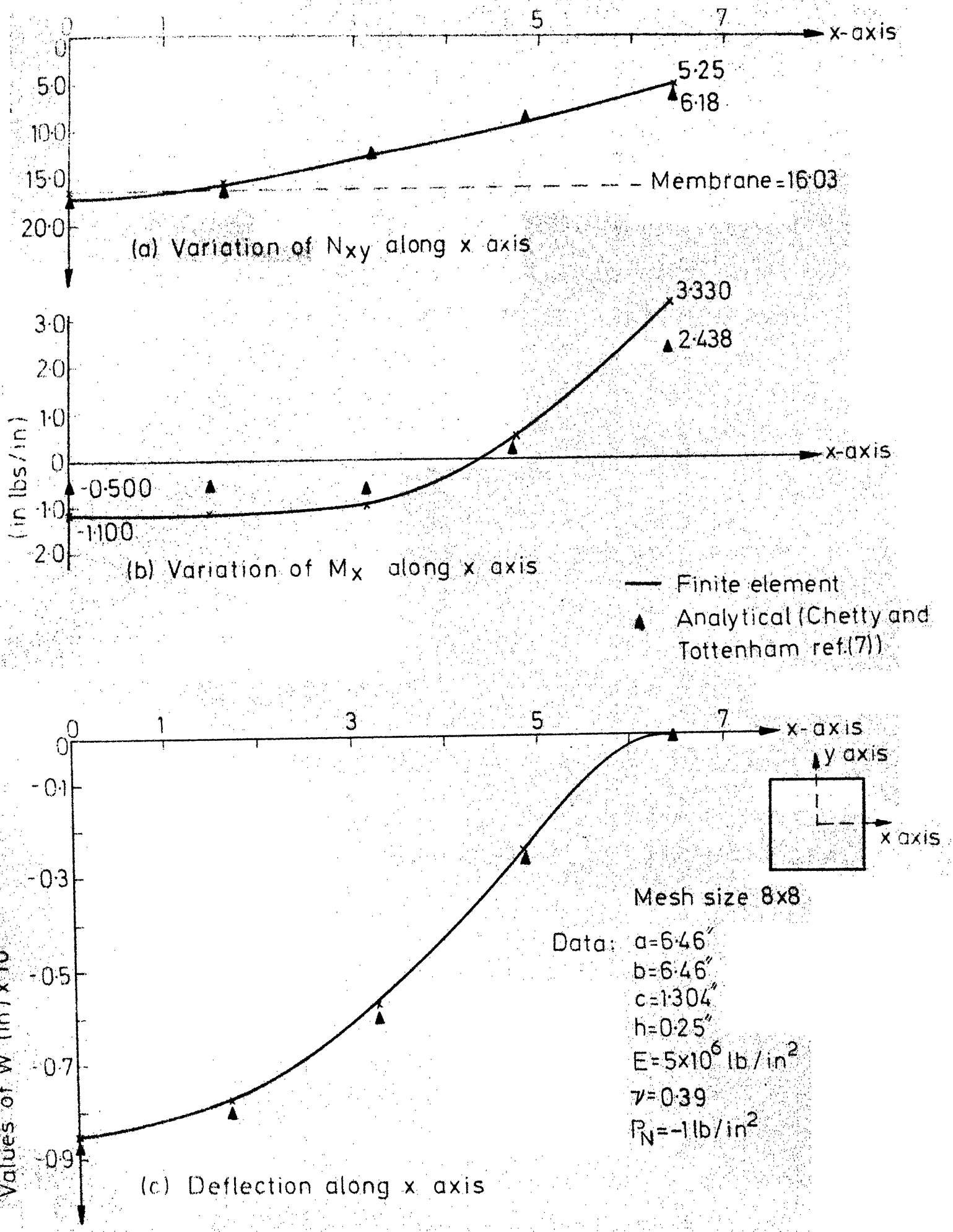

FIG. 3.2 HYPERBOLIC PARABOLID SHELL WITH FIXED EDGES UNDER UNIFORM NORMAL LOAD

Displacement boundary conditions for an edge X = constant are:

$$u = 0$$
$$v = 0$$
$$w = 0$$
$$\beta_1 = 0$$
$$\beta_2 = 0$$

Similar boundary conditions are used for an edge Y = constant.

The figure shows the comparison of the finite element analysis with those given in (7). This agreement is quite good considering the size of the grid used in the finite element analysis. This is in agreement with the fact that there would be improvement of accuracy when the boundary conditions as in this case are all of the forced type. It is interesting to note that the agreement is better for the membrane shear force N_{XY} than for the bending moment M_X.

The membrane shear N_{XY} exceeds the membrane value of 16.0 lbs/sq.in. by only a slight amount at the centre of the shell, but the bending moment propagates into the central region of the shell, producing fairly large bending stresses. The maximum deflection at the centre of the shell is 8.732×10^{-3} in. The maximum deflection at the centre of the shell with knife edge supports (26) is 9.18×10^{-3} in. The displacement boundary conditions at X = constant are :

$$u = 0$$
$$w = 0$$
$$\beta_2 = 0$$

Similar boundary conditions are used for an edge Y = Constant. It is seen that the central deflection of a knife edge supported shell is about 1.14 times that of the shell with all edges clamped whereas inplates it is about 3.3 (85).

3.3.2 Figure 3.3 shows a square hyperbolic paraboloid clamped on all edges and subjected to a uniform normal load of -0.1 Kg/sq.cm. This shall has been analysed by Connor and Brebbia (24).

Shell Data:

a = 50 cm E = 28,500 Kg/sq.cm

b = 50 cm ν = 0.4

c = 10 cm

h = 0.8 cm

A grid size of (8x8) over the entire shell is used in the analysis.

Displacement boundary conditions for an edge X = constant are:

u = 0

v = 0

w = 0

β_1 = 0

β_2 = 0

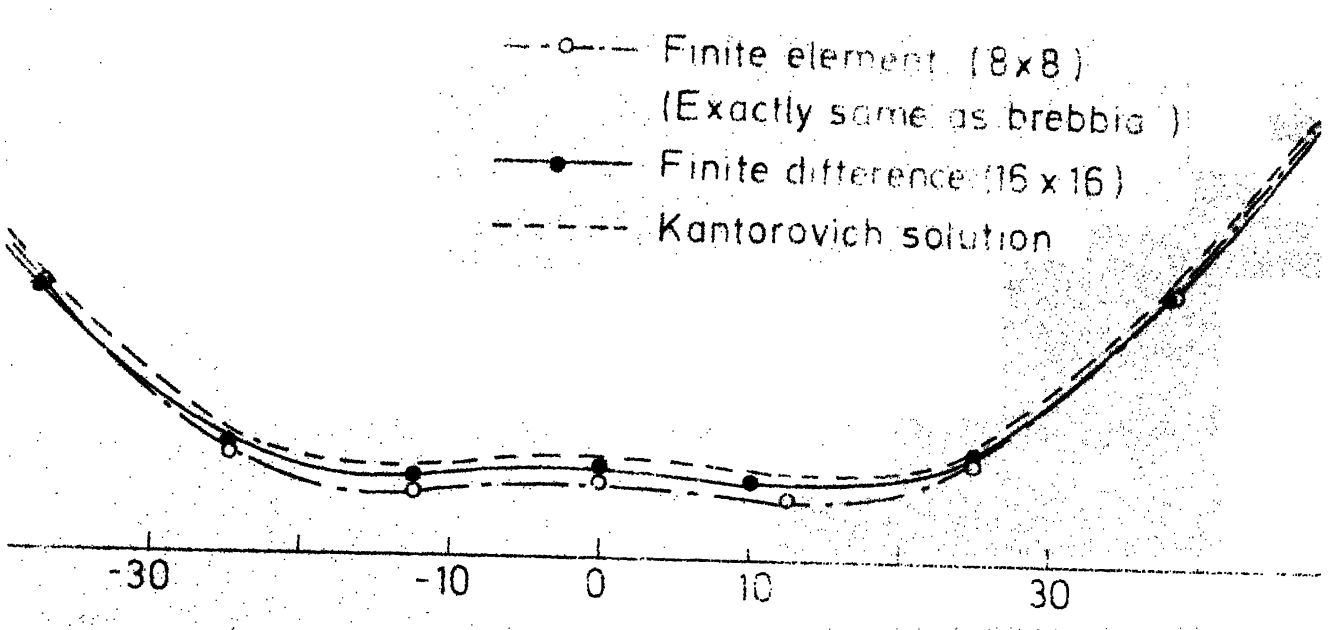

NORMAL DEFLECTION AT CENTER LINE CLAMPED HYPAR UNDER UNIFORM NORMAL LOAD

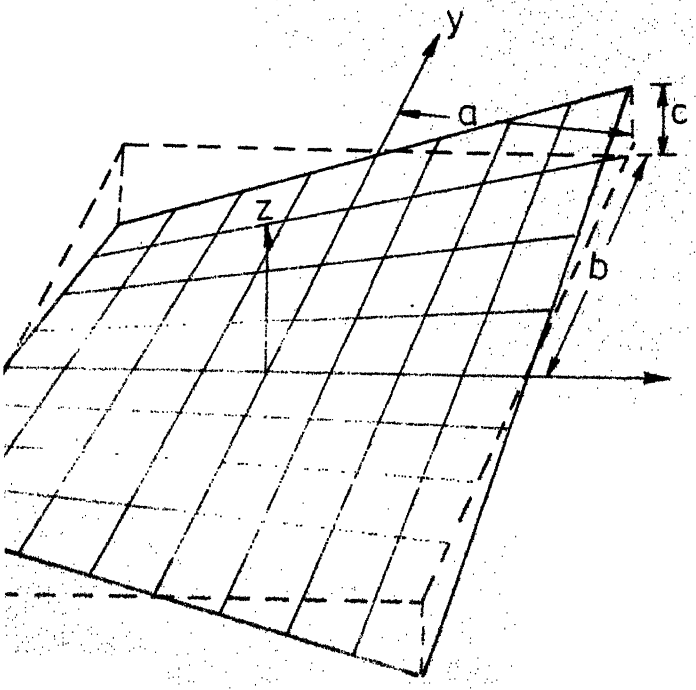

Mesh size 8x8

Data:

a = 50 cm

b = 50 cm

$E = 28{,}500\ kg\ cm^{-2}$

$P_N = 0{\cdot}1\ kg\ cm^{-2}$

c = 10 cm

h = 0·8 cm

$\nu = 0{\cdot}4$

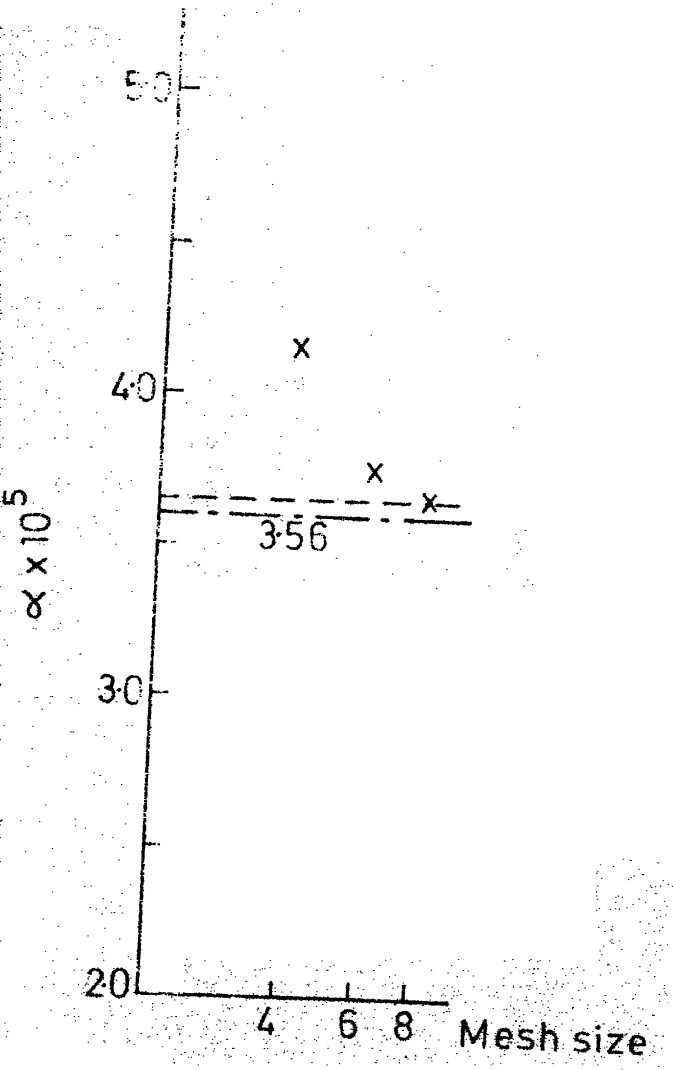

— — KANT & GALERKIN (Ref: 7)

—·— FINITE DIFF (Ref: 67)

$$W_c = \alpha \frac{P_N (2a)^4}{D}, \quad D = \frac{E t^3}{12 (1-\nu^2)}, \quad \nu = 0.4$$

W_c = Central deflection at $x=0$, $y=0$

FIG. 3.4 COMPARISON OF CENTRAL DEFLECTION CLAMPED HYPAR

Similar boundary conditions are used for an edge Y = constant.

The Figure 3.4 shows a comparison of the finite element results for the normal displacement at the centre with the values obtained using the Kantorovich-Galerkin procedure (7) and second order finite differences (67).

The variation of normal displacement at the centre line (Y = 0) with mesh size is plotted in Figure 3.3. Close agreement is obtained with a finite element mesh size (8x8) equal to twice the finite difference grid spacing (16x16), the percentage difference is less than 4 percent for the central deflection. By finer mesh size, the finite element solutions may be made to agree within 1 percent at all points.

The comparison of results shows that one can obtain good results with the finite element method using a reasonably coarse mesh and fairly simple displacement expansions which are not compatible and which do not include all the rigid body displacement terms.

CHAPTER 4

SOLUTION FOR LARGE DEFLECTION OF CLAMPED HYPERBOLIC PARABOLOID SHELL BOUNDED BY STRAIGHT EDGES

4.1 APPLICATION TO HYPERBOLIC PARABOLOID BOUNDED BY ITS CHARACTERISTICS

In order to demonstrate the capability of the finite element formulation presented earlier, a clamped hypar shell bounded by its characteristic lines is chosen. The Newton-Raphson method has been employed to trace the load-deflection curve. Since the computer memory is limited, a 4x4 mesh size is taken. The tangent stiffness matrix is evaluated by numerical integration method using Gauss-Legendre quadrature. The load-deflection curve is drawn for the centre of the shell. The nondimensional parameters used are

$$\mu = a(12(1-\nu^2))^{1/4}/(4tR)^{1/2}$$

$$\bar{w} = w/t \qquad (4.1)$$

$$\bar{Q} = P_N R^2/Et^2$$

$$\nu = 0.4$$

where a is the dimension of the square planform along X-axis, R is defined by the surface equation of the shell $Z = XY/R$.

For the shell under consideration

$$R = \frac{a \times a}{h} = 250$$

$$t = 0.8$$

$$\nu = 0.4$$

$$\frac{R}{t} = 312.5$$

$$\mu = 3.15$$

$$\bar{Q} = P_N R^2/Et^2 = 3.247\ P_N$$

4.2 DISCUSSION OF THE RESULT

For the buckling of the shell, experimental results as shown in Figure 4.1 give a value of 0.338 Kg/cm^2 (6-7). Buckling is considered to occur when the behaviour changes abruptly, i.e., when there is a sudden change in the load-deflection behaviour. Figure 4.1 indicates buckling load as 0.48 Kg/cm^2. The only rigorous mathematical equation for predicting the buckling load of an ideal hyperbolic paraboloid, simply supported on the perimeter, was derived by Reissner (3), namely

$$P_{N\ cr} = \frac{2Et^2\ h^2}{3(1-\nu^2)^{1/2} a^2 b^2} \qquad (4.2)$$

where $P_{N\ cr}$ = the magnitude of the uniformly distributed load that causes buckling. Equation (4.2) is most significant because it establishes the functional

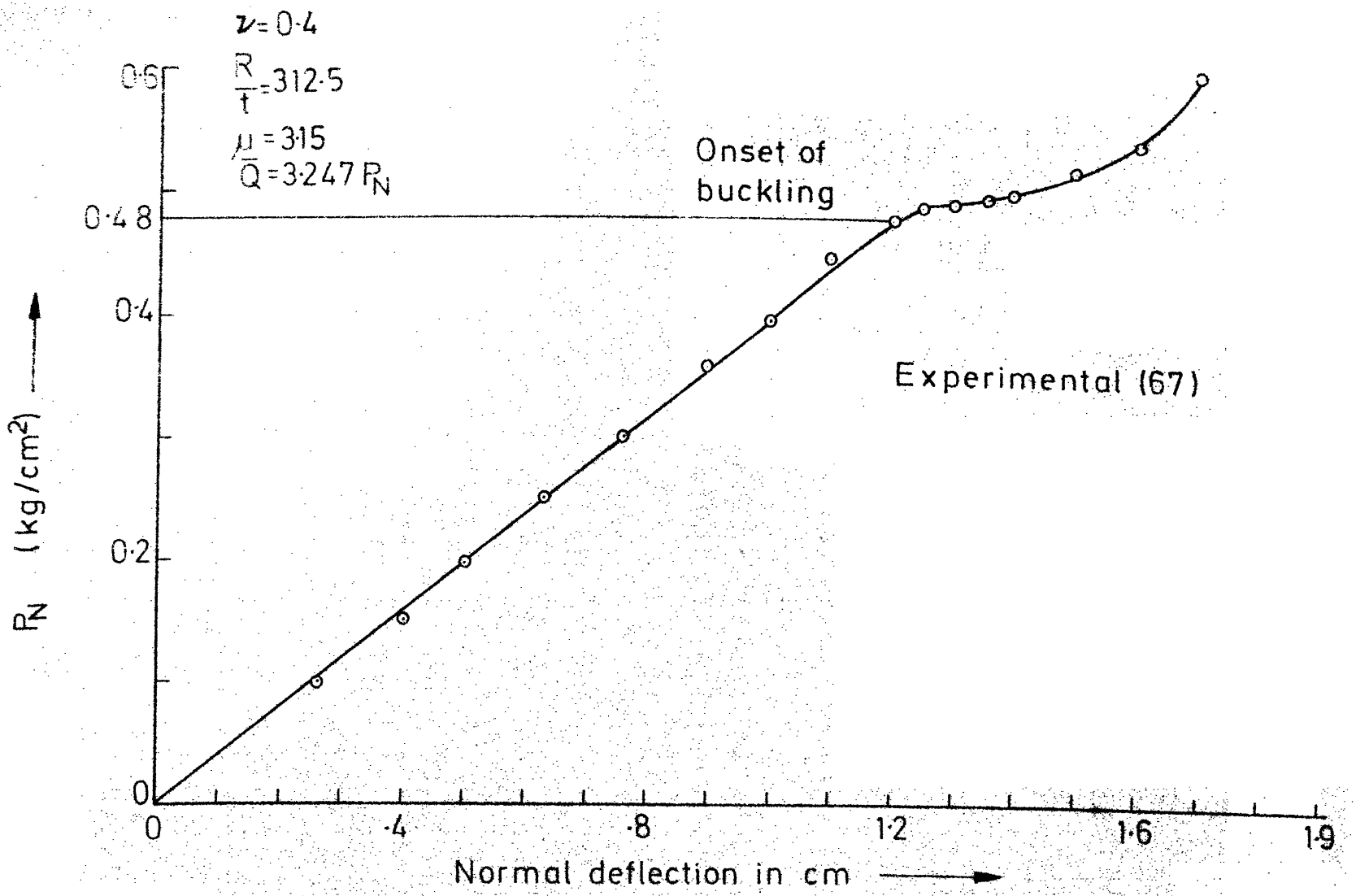

FIG. 4·1 LOAD DEFLECTION CURVE AT THE CENTRE OF THE SHELL

relationship between the buckling load and the pertinent shell and material variables. The form of the half-wave length of buckle, ℓ_η, is given by

$$\ell_\eta = \frac{\pi}{2^4 \{3(1-\nu^2)\}^{1/2}} (ab)^{1/2} \left(\frac{t}{h}\right)^{1/2} \qquad (4.3)$$

and is physically interpreted by Reissner to represent a 'wrinkling' of shell in the direction of the compression diagonal. Reissner's analysis based on simply-supported boundary conditions gives (lower critical load. The experimental, finite-element and theoretical (Reissner's linearized stability analysis) values of buckling load are compared in Table 4.1.

Table 4.1

Experimental (67) 1	Finite element (4x4) 2	Reissner (3) 3
0.338	0.480	0.380

The experimental result gave lower value due to imperfections and the probable lack of complete translational fixity at the boundary. The computation has been done on IBM 375/155 Computer at I.I.T. Madras.

4.3 EXPERIMENTAL CONCLUSIONS OF LEET (68)

Some of the experimental conclusions of Leet (68) on the study of stability in the hyperbolic paraboloid bounded by characteristics are mentioned below.

A) Buckling of a fixed edge hyperbolic paraboloid is characterized by the entire surface of the shall forming ripples in the direction of the compression diagonal.

B) At the critical load, the hyperbolic paraboloid surface undergoes a sudden bend or knee in the load-deflection curve.

C) If sufficient edge member stiffness is present to prevent buckling of edge members before the shell buckles, it seems that the buckling load that a shell can develop may be related to the edge member axial stiffness withma limited range.

D) The hyperbolic paraboloid with fixed edge boundaries and loaded by air pressure, buckles into half-waves whose half-length is closely predicted by equation (4.3).

E) Imperfections reduce the magnitude of the initial buckling load. In the air pressure tests, the buckling load varied from approximately 51 percent to 71 percent of the load given by equation (4.2). The larger the imperfections, the lower the initial buckling load.

F) After initial buckling wave formation has occurred, the shell develops a tension field mode to carry additional load.

G) The ultimate load of the shell and edge member system is shown to be dependent on the edge member moment of inertia, I_{XX}, provided sufficient area is present to prevent yielding of the material and no local instability occurs.

H) The ultimate load of a hyperbolic paraboloid is dependent on the manner of support of the edge beams. The shell whose edge members are fixed at one end and simply supported at the other end carried more load than the shell whose edge members are fixed at one end only.

CHAPTER 5

CONCLUSIONS AND DISCUSSION

5.1 CONCLUSIONS

The finite element as herein applied to shallow shells, using elements of the same shape as the shell middle surface rather than a series of flat elements has been shown to give results in good agreement with exact solutions. The most advantageous feature of the method is its versatility and the ease with which, for example, various boundary conditions (including elastic edge beams) can be included.

It is found that inclusion of complete rigid body motion in the displacement function makes no change in the results obtained in the case of hyperbolic paraboloid shells bounded by characteristics with clamped edges from those obtained without inclusion of complete rigid body motion (4).

It is also reported (82) that Birkhoff-Garabedian interpolation formula which ensures compatibility i.e., the continuity of derivatives of the normal displacement across inter-element boundaries has not been essential as the results agreed with those obtained violating compatibility.

Some of the peculiarities of the finite element results, notably the under-estimation of the membrane forces near the boundary, may be traced to the fact that the natural boundary conditions are not exactly satisfied for a finite grid size. In a problem for which the exact solution is not known, the degree of satisfaction of the natural boundary conditions may be used as a practical method of assessing whether or not a fine enough grid has been used in the analysis.

5.2 SCOPE FOR FURTHER WORK

1) The improvement of the satisfaction of the natural boundary condition involves displacement shapes which are capable of satisfying, for example, the membrane natural boundary conditions. This, however, would result in an increased number of generalized coordinates per element and thus for the same computational effort, not as fine a mesh could be used. Therefore, whether or not improved accuracy should be sought by using more redefined displacement assumptions, or by using relatively crude assumptions together with fine grids is answerable only by actual numerical comparisons.

Alternative methods of satisfying the natural boundary conditions are the use of Lagrangian multipliers (64) or a reformulation as a mixed variational problem in which some of the displacements and some of the stresses are assumed in terms of generalized coordinates (58,71).

2) Several extensions of the scope of this investigation suggest themselves. Temperature effects, non-uniform thickness, anistropy, and flexible column supports could all be immediately included.

Other extensions, such as to creep, vibrations, buckling (both pre- and post-) and plasticity could also be made.

3) Skewed and tilted hyperbolic paraboloid shells should also be brought within the purview of finite element method.

4) It is necessary to develop a deep shell element using discrete Kirchhoff assumptions and shear strain displacement relations. Noteworthy start has been made by Gurbachan Dhatt and Jean-Louis Batoz (87) by developing a deep triangular shell element. Deep shells may necessitate the consideration of wind loads in addition to gravity loads.

5) Thick shells are still a challenge. The straightforward use of the three-dimensional concept offers certain difficulties. In the first place the retention of three degrees of freedom at each node leads to large stiffness coefficients for relative displacements along an edge corresponding to the shell thickness. This presents numerical problems and may lead to ill-conditioned

equations when shell thicknesses become small compared with other dimensions in the element. The second factor is that of economy. The use of several nodes across the thickness ignores the well-known fact that even for thick shells the 'normals' to the middle surface remain practically straight after deformation. Thus an unnecessarily high number of degrees of freedom has to be carried, involving penalties of computer time. Shear deformations are an important feature in the thick shell situations. Special isoparametric curved hexahedron three-dimensional element has to be fully developed and exploited. They are already proved to be better than tetrahedron elements. Obviously numerical integration methods come in handy. For axi-symmetric shells the formulation is obviously simplified as the mid-surface is defined by only two coordinates ξ, η and a considerable saving in computer effort is obtained. Spherical domes, edge loaded cylinder, cooling towers and curved dams require the thick shell analysis.

REFERENCES

1. Margeurre, K., 'Zur Theorie der gekrümmten Platte grösser Formanderung', Proceedings, Fifth International Congress on Applied Mechanics, 1938.
2. Vlasov, V.Z., 'General Theory of Shells and its Applications in Engineering', NASA Technical Translation, F-99.
3. Reissner, E., 'On Some Aspects of the Theory of Thin Elastic Shells', Journal, Boston Society of Civil Engineers, 1955.
4. A.peland, K., 'Stress Analysis of Translational Shells', Journal of the Engineering Mechanics Division, ASCE, February, 1961.
5. Bouma, A.L., 'Some Applications of the Bending Theory regarding Doubly Curved Shells', Proceedings of the Symposium on the Theory of Thin Elastic Shells, August 1956.
6. Flugge, W. and Conrad, D.A., 'A Singular Solution in the Theory of Shallow Shells', Technical Report 101, Division of Engineering Mechanics, Stanford University, Sept. 1956.
7. Chetty, S.M.K. and Tottenham, H., 'An Investigation into the Bending Analysis of Hyperbolic Paraboloid Shells', Indian Concrete Journal, July 1964.
8. Gustafson, W.C. and Schnobrich, W.C., 'Multiple Translational Shells', IASS-IMCYC Congress, Intenacional Sobre La Application de Estructuras Laminaus en Arquitctura, Mexico City, September 1967.

9. Das Gupta, N.C., 'Edge Disturbances in a Hyperbolic Paraboloid', Civil Engineering and Public Works Review, February 1963.

10. Soare, M., 'A Numerical Approach to the Bending Theory of Hypar Shells', Indian Concrete Journal, February-March 1966.

11. Mirza, J.F., 'Stresses and Deformations in umbrella Shells', Journal of the Structural Division, ASCE, April 1967.

12. Russell, R.R., and Gerstle, K.H., 'Bending of Hyperbolic Structures', Journal of the Structural Division, ASCE, 1967.

13. Russell, R.R. and Gerstle, K.H., 'Hyperbolic Paraboloid Structures on Four Supports', Journal of the Structural Division, ASCE, 1968.

14. Abu-Sitta, S.H., 'Finite Difference Solutions of the Bending Theory of the Elliptic Paraboloid', IASS Bulletin No. 20.

15. Schnobrich, W.C., 'A Physical Analogue for the Numerical Analysis of Cylindrical Shells,' Ph.D. Thesis, University of Illinois, 1962.

16. Mohraz, B. and Schnobrich, W.C., 'The Analysis of Shallow Shell Structures by a Discrete Element System', Civil Engineering Studies, SRS 304, University of Illinois, March, 1966.

17. Parikh, K.S., 'Analysis of Shells using Framework Analogy', Sc.D. Thesis, Massachusetts Institute of Technology, June 1962.

18. Clough, R.W., 'The Finite Element Me-thod in Structural Mechanics', Stress Analysis, Edited by O.C.Zienkiewicz and G.S.Hollister, Wiley, 1965.

19. Zienkiewicz, O.C. and Cheung, Y.K., 'The Finite Element Method for Analysis of Elastic Isotropic and Orthotropic Slabs', Proceedings, Institution of Civil Engineers, August 1964.

20. Melosh, R.J., 'Basis for Derivation of Matrices for the Direct Stiffness Method', AIAA Journal, July, 1963.

21. Chu, T.C. and Schnobrich, W.C., 'Finite Element Analysis of Translational Shells', Computers and Structures, Vol.2, 1972.

22. Jones, R.E. and Strome, D.R., 'A Survey of the Analysis of Shells by the Displacement Method', Proceedings, Conference on Matrix Methods in Structural Mechanics, WPAFB, Ohio, 1965.

23. Strickl in, J., Navaratna, D.R. and Pian, T.H.H., 'Improvements on the Analysis of Shells of Revolution by the Matrix Displacement Method', Technical Note, AIAA Journal, November 1966.

24. Connor, J.J. and Brebbia, C., 'Stiffness Matrix for Shallow Rectangular Shell Element', Journal of Engineering Mechanics Division, ASCE, October 1967.

25. Dhatt, G., 'Numerical Analysis of Thin Shells by Curved Triangular Elements based on Discrete Kirchhoff Hypothesis' Proceedings, Symposium on Application of Finite Element Methods in Civil Engineering, Vanderbilt University, 1969.

26. Pecknold, D.A.W. and Schnobrich, W.C., 'Finite Element Analysis of Skewed Shallow Shells', Journal of Structures Division, ASCE, April 1969.

27. Kovach, L.D., 'Life can be so nonlinear', American Scientist, Vol.48, 1960.

28. Martin, H.C., 'Finite Element Formulation of Geometrically Nonlinear Problems', Recent Advances in Matrix Methods of Structural Analysis and Design, R.H. Gallaghar, et al, Ed. University of Alaba ma Press, 1971.

29. Oden, J.T., 'Finite Element Applications in Nonlinear Structural Analysis', Proc. of Symposium on Application of Finite Element Methods in Structural Engineering, W. Rowan and R. Hackett, Eds., Vanderbilt University, Nashville, Tenn., 1969.

30. Stricklin, J.A., Haisler, W. and Von Riesemann, W., 'Formulation, Computation and Solution Procedures for Material and/or Geometric Nonlinear Structural Analysis by the Finite Element Method', Sandia Corp. Report SC-CR-73-3102, Albuquerque, N.M., 1972.

31. Mallett, R. and Marcal, P., 'Finite Element Analysis of Nonlinear Structures', Journal of the Structural Division, ASCE, 94, No. ST9, September 1968.

32. Wissman, J.W., 'Nonlinear Structural Analysis: Tensor Formulations', Proceedings of (First) Air Force Conference on Matrix Methods in Structural Mechanics, AFFDL-TR66-80, 1965.

33. Bogner, F., Fox R.L., and Schmit, L., 'Finite Deflection Analysis using Plates and Shell Discrete Elements', AIAA J, 6, No.5, May 1968.

34. Oden, J.T. and Key, J.E., 'Numerical Analysis of Finite Axisymmetric Deformation of Incompressible Solids of Revolution', International Journal of Solids and Structures, Vol.6, No.5, May, 1970.

35. Broyden, C.G., 'Quasi-Newton-Methods and their Application to Function Minimization', Maths. Comp., 21, 1967.

36. Mau, S. and Gallagher, R.H., 'A Finite Element Procedure for Nonlinear Prebuckling and Initial postbuckling Analysis', NASA CR-1936, January 1972.

37. Roberts, T.M. and Ashwell, D.C., 'The use of Finite Element Midincrement Stiffness Matrices in the Post-buckling Analysis of Imperfect Structures' Int. J. Solids Struct. 7, 1971.

38. Hofmeister, L.D., Greenbaum, G. and Evenson, D., 'Large Strain, Elastic Plastic Finite Element Analysis', AIAA J., 9, No.7, July 1971.

39. Pian, T.H.H. and Tong Pin, 'Variational Formulation of Finite-Displacement Analysis', Proceedings of IUTAM Symposium on High Speed Computing of Elastic Structures, Liege, 1970.

40. Fellippa, C., 'Refined Finite Element Analysis of Linear and Nonlinear Two-Dimensional Structures', Report SESM 66-22, Struct. Engrg Lab., Univ. of California, Berkeley, October 1966.

41. Zienkiewicz, O.C. and Nayak, G.C., 'A General Appraoch to Problems of La-rge Deformations and Plasticity using Isoparametric Elements', Proc. of Third Air Force Conf. on Matrix Methods in Struct.Mech., Drayton, Ohio, 1971.

42. Dupuis, G.A., Pfaffinger, D. and Marcal, P.V., 'Effective Use of the Incremental Stiffness Matrices in Nonlinear Geometric Analysis', IUTAM Symposium on High Speed Computing of Elastic Structures, Liege, Belgium, 1970.

43. Walker, A.C., 'A Nonlinear Finite Element of Shallow Circular Arches', Int. J. Solids Struct., 5, 1969.

44. Morin, N., 'Nonlinear Analysis of Thin Shells', Report R70-43, Dept. of Civil Engineering, M.I.T., 1970.

45. Barsoum, R.S., 'Finite Element Methods Applied to the Problem of Stability of a Non-conservative System', Int.J. for Num. Methods in Engineering, 3, 1971.

46. Bronlund, O., 'Eigenvalues of Large Matrices' Proc. of ISD/ISSC Symp. on Finite Element Techniques', Stuttgart, June 1969.

47. Whetstone, W. and Jones, C.E., 'Vibrational Characteristics of Linear Space Frames', Journal of the Structural Division, ASCE, 95, 1969.

48. Rosen, R. and Rubenstein, M., 'Substructure Analysis by Matrix Decomposition', Journal of the Structural Division, ASCE, 95, 1969.

49. Dong, S.B., Wolf, J. and Peterson, F., 'On a Direct Iterative Eigensolution Technique', Int. J. for Numerical Methods in Engineering, 4, No.2, 1972.

50. Hestenes, M. and Stiefel, E., 'Method of Conjugate Gradients for Solving Linear Systems', Journal of Research, NBS, 49, 1952.

51. Kerr, A.D. and Soifer, M.T., 'The Linearization of the Pre-buckling State and Its effects on the Determined Instability Load', Trans. ASME, J. of Applied Mech., 36, 1969.

52. Haftka, R.T., Mallett, R.H. and Na chbar, W., A Koiter-Type Method for Finite Element Analysis of Nonlinear Structural Behaviour', AFFDL TR 70-130, Vol.1, November, 1970.

53. Murray, D. and Wilson, E., 'Finite Element Large Deflection Analysis of Plates', Journal of Engineering, Mech. Div., ASCE, 95, No. EM1, February, 1969.

54. Almroth, B.O., and Brogan, F.A., 'Bifurcation Buckling as an Approximation of the Collapse Load for General Shells', AIAA J., 10, No.4, April 1972.

55. Oden, J.T., 'Some Results of Finite Element Applications in Nonlinear Elasticity', Nat. Symp. on Computerised Structural Analysis and Design, G.Washington Univ., March 1972.

63. Clough, R.W. and Tocher, J.L., 'Finite Element Stiffness Matrices for Analysis of Plate Bending', Conf. on Mat. Methods in Struct. Mech., W-FAFB, Ohio, October 1965.

64. Haisler, W.E. and Strickl in, J.A., 'Rigid Body Displacements of Curved Elements in the Analysis of Shells by the Matrix Displacement Method', Technicalk Note, AIAA Journal, August 1967.

65. Jones, R.E., 'A Generalization of the Direct Stiffness Method of Structural Analysis', AIAA Journal, May 1964.

66. Turner, M.J., Dill, E.H., Martin, H.C. and Melosh, R.J., 'Large Deflection of Structures subjected to Heating and External Loads', Journal of Aerospace Services, Vol.27, February 1960.

67. Brebbia, C., 'On Hyperbolic Paraboloid Shells', Ph.D. Thesis, University of Southampton, England, September 1967.

68. Leet, K.M., 'Study of Stability in the Hyperbolic Paraboloid', Journal of Engineering Mechanics Div., ASCE, Vol. 92, No. EM1, February 1966.

69. Scordelis, A.C. and Lo, K.S., 'Computer Analysis of Cylindrical Shells', ACI Journal, Proc. 61(5), 1964.

70. Long, J.E., 'Experimental Investigation of the Effect of Edge Stiffening on a Square Hyperbolic Paraboloid Shell', Technical Report, Cement and Concrete Association, England, December 1966.

71. Schnobrich, W.C., Mohraz, B. and Hoebel, J.L., 'Influence of Edge Beam Properties on the Stress in Hyperbolic Parabolus', IASS International Colliquium on Progress of Shell Structures in the Last Ten Years, Madrid, 1969.

72. Pian, T.H.H., 'Derivation of Element Stiffness Matrices by Assumed Stress Distributions', AIAA Journal, 2(7), 1964.

73. Pian, T.H.H. and Tong, P., 'Rationalization in Deriving Element Stiffness by Assumed Stress Approach', Proc. 2nd C onference on Matrix Methods in Structural Mechanics, AFFDL-TR-68-150, WPAFB, Ohio, 1968.

74. Pirotin, S.D., 'Incremental Large Deflection Analysis of Elastic Structures', Ph.D. Thesis, M.I.T. Department of Aeronautics and Astronautics, 1971.

75. Pian, T.H.H., 'Hybrid Models', Int. Symposium on Numerical and Computer Methods in Structur-al Mechanics, Univ. of Illinois, Urbana, September 1971.

76. Satyanadham, Atluri, 'On the Hybrid Stress Finite Element Models for Incremental Analysis of Large Deflection Problems', Int. Journal of Solids Structures, Vol.9, No.10, October 1973.

77. Fried, I., 'Discretization and Round-off Errors in the Finite Element Analysis of Boundary Value Problems and Eigenvalue Problems', Ph.D. Thesis, M.I.T., 1971.

78. _____., 'Discretization and Round-Off Errors in Higher Order Finite Elements', AIAA Journal 9, 1971.

79. _____., 'The l_2 and l_∞ Condition Numbers of the Finite Element Stiffness and Mass Matrices and Their Pointwise Convergence', Conference on the Mathematics of Finite Elements and Applications, Brunel University, 1972.

80. _____, 'Condition of the Finite Element Stiffness Matrices Generated from Nonuniform Meshes', AIAA Journal, 10, 1972.

81. Kabaila, A.P. and Beckers, P., 'Computer Integration of Congruently Transformed Matrices', UNICIV Report No. R-75, October 1971.

82. Birkhoff, G. and Garabedian, H.L., 'Smooth Surface Interpolation', Journal of Mathematics and Physics, Vol. 39, 1960.

83. Ramaswamy, G.S., 'Design and Construction of Concrete Shell Roofs', Tata McGraw-Hill Publishing Company Ltd. Bombay.

84. Gallagher , R.H., Gellatly, R.A., Padlog, J. and Mallet, R.H., 'A Discrete Element Procedure for Thin Shells in Stability Analysis', AIAA Journal, Vol.5, No.1, pp.138-145, January, 1967.

85. Timoshenko, S.P. and Woinowsky-Krieger, S., 'Theory of Plates and Shells', McGraw-Hill Co., London.

86. Schmit, L.A., Bogner, F.K. and Fox, R.L., 'Finite Deflection Structural Analysis using Plate and Cylindrical Shell Discrete Elements', Proceedings, AIAA/ASME 8th Structures, Structural Dynamics and Materials Conference, Palm Springs, California, 29-31 March 1967, pp. 197-211.

87. Gurabachan Dhatt, and Jean - Louis Batoz, 'Buckling of Deep Shells', Second International Conference 'Structural Mechanics in Reactor Technology', Berlin, Germany, September 1973.

APPENDIX A

NUMERICAL INTEGRATION USING GAUSS-LEGENDRE QUADRATURE

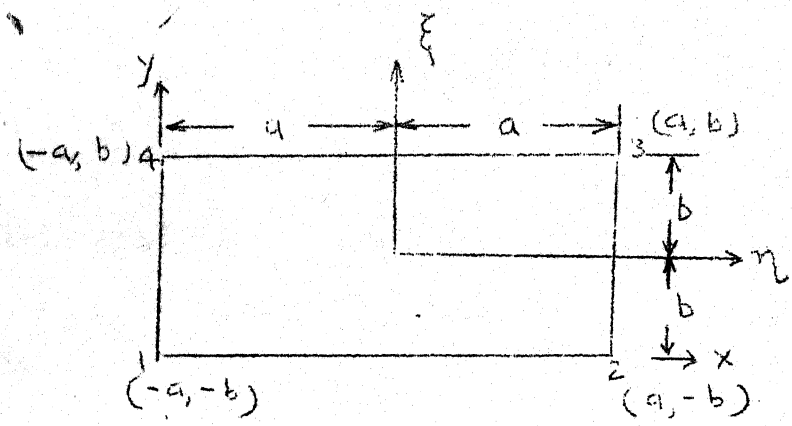

Figure A.1: Normalized Coordinates for a Rectangle.

$$u = \alpha_1 + \alpha_2 X + \alpha_3 Y + \alpha_4 XY \qquad (A.1)$$

Substituting the nodal coordinates in the above

$$\{u\}^e = \begin{bmatrix} 1 & -a & -b & ab \\ 1 & a & -b & -ab \\ 1 & a & b & ab \\ 1 & -a & b & -ab \end{bmatrix} \{\alpha\}^e$$

$$= [A]\{\alpha\}^e \qquad (A.2)$$

$$u = [1\ X\ Y\ X\ Y]\,[A]^{-1}\{u\}^e \qquad (A.3)$$

Simplyfying the R.H.S.,

$$u = \left[\frac{1}{4}\left(1-\frac{X}{a}\right)\left(1-\frac{Y}{b}\right) \frac{1}{4}\left(1+\frac{X}{a}\right)\left(1-\frac{Y}{b}\right) \frac{1}{4}\left(1+\frac{X}{a}\right)\left(1+\frac{Y}{b}\right) \right.$$

$$\left. \frac{1}{4}\left(1-\frac{X}{a}\right)\left(1+\frac{Y}{b}\right)\right] \{u\}^e \qquad (A.4)$$

Let $\xi = \frac{X}{a}$

$\eta = \frac{Y}{b}$

$$u = \left[\frac{1}{4}(1-\xi)(1-\eta) \frac{1}{4}(1+\xi)(1-\eta) \frac{1}{4}(1+\xi)(1+\eta) \frac{1}{4}(1-\xi)(1+\eta)\right]\{u\}^e \qquad (A.5)$$

Similarly

$$v = \left[\frac{1}{4}(1-\xi)(1-\eta) \frac{1}{4}(1+\xi)(1-\eta) \frac{1}{4}(1+\xi)(1+\eta) \frac{1}{4}(1-\xi)(1+\eta)\right]\{u\}^e \qquad (A.6)$$

$$w = A_1 + A_2X + A_3Y + A_4X^2 + A_5XY + A_6Y^2 + A_7X^3 + A_8X^2Y$$

$$+ A_9XY^2 + A_{10}Y^3 + A_{11}X^3Y + A_{12}XY^3$$

$$\beta_1 = \frac{1}{a}\frac{\partial w}{\partial X}$$

$$= -1/a\left[A_2 + 2A_4X + A_5Y + 3A_7X^2 + 2A_8XY + A_9Y^2 + 3A_{11}X^2Y + A_{12}Y^3\right] \qquad (A.7)$$

$$\beta_2 = -\frac{1}{b}\frac{\partial w}{\partial Y}$$

$$= -\frac{1}{b}\left[A_3 + A_5X + 2A_6Y + A_8X^2 + 2A_9XY + 3A_{10}Y^2 + A_{11}X^3 + 3A_{12}XY^2\right]$$

Substituting the nodal coordinates of the element in the above,

$$\{w\}^e = [C]\{A\} \qquad (A.8)$$

or

$$\{A\} = [C]^{-1}\{w\}^e \qquad (A.9)$$

$$\therefore w=[1\ \xi\ \eta\ \xi^2\ \xi\eta\ \eta^2\ \xi^3\ \xi^2\eta\ \xi\eta^2\ \eta^3\ \xi^3\eta\ \xi\eta^3]\ [C]^{-1}\{w\}^e$$

or

$$w = [N_1\ N_2\ N_3\ N_4\ N_5\ N_6\ N_7\ N_8\ N_9\ N_{10}\ N_{11}\ N_{12}]\ \{w\}^e \qquad (A.11)$$

where N_1 to N_{12} are polynomials in ξ, η.

For a two-dimensional strain-displacement relationship, we need to know $\frac{\partial u}{\partial X}$ etc. These are not directly available and hence a relationship between X,Y and ξ, η must be established. By partial differentiation

$$\begin{Bmatrix} \frac{\partial u}{\partial \xi} \\ \\ \frac{\partial u}{\partial \eta} \end{Bmatrix} = \begin{bmatrix} \frac{\partial X}{\partial \xi} & \frac{\partial Y}{\partial \xi} \\ \\ \frac{\partial X}{\partial \eta} & \frac{\partial Y}{\partial \eta} \end{bmatrix} \begin{Bmatrix} \frac{\partial u}{\partial X} \\ \\ \frac{\partial u}{\partial Y} \end{Bmatrix}$$

$$= [J] \begin{Bmatrix} \frac{\partial u}{\partial X} \\ \frac{\partial u}{\partial Y} \end{Bmatrix} \quad \text{where } [J] \text{ is aJacobian matrix} \qquad (A.12)$$

$$\therefore \begin{Bmatrix} \frac{\partial u}{\partial X} \\ \frac{\partial u}{\partial Y} \end{Bmatrix} = [J]^{-1} \begin{Bmatrix} \frac{\partial u}{\partial \xi} \\ \frac{\partial u}{\partial \eta} \end{Bmatrix} \qquad (A.13)$$

The relationship between the normal and global cartesian coordinates is given by:

$$X = \frac{1}{4}(1-\xi)(1-\eta)X_1 + \frac{1}{4}(1+\xi)(1-\eta)X_2 + \frac{1}{4}(1+\xi)(1+\eta)X_3 + \frac{1}{4}(1-\xi)(1+\eta)X_4 \qquad (A.14)$$

$$Y = \frac{1}{4}(1-\xi)(1-\eta)Y_1 + \frac{1}{4}(1+\xi)(1-\eta)Y_2 + \frac{1}{4}(1+\xi)(1+\eta)Y_3 + \frac{1}{4}(1-\xi)(1+\eta)Y_4 \qquad (A.14)$$

The Jacobian matrix for the above becomes

$$[J] = \begin{bmatrix} a/2 & 0 \\ 0 & b/2 \end{bmatrix} \qquad (A.15)$$

$$|J| = \frac{ab}{4} \qquad (A.16)$$

$$[J]^{-1} = \begin{bmatrix} 2/a & 0 \\ 0 & 2/b \end{bmatrix}$$

$$\therefore \begin{Bmatrix} \frac{\partial u}{\partial X} \\ \\ \frac{\partial u}{\partial Y} \end{Bmatrix} = \begin{Bmatrix} \frac{2}{a} & \frac{\partial u}{\partial \xi} \\ \\ \frac{2}{b} & \frac{\partial u}{\partial \eta} \end{Bmatrix} \qquad (A.17)$$

or

$$\begin{Bmatrix} \frac{\partial}{\partial X} \\ \\ \frac{\partial}{\partial Y} \end{Bmatrix} = \begin{Bmatrix} \frac{2}{a} & \frac{\partial}{\partial \xi} \\ \\ \frac{2}{b} & \frac{\partial}{\partial \eta} \end{Bmatrix} \qquad (A.18)$$

$$\begin{Bmatrix} \frac{\partial^2 w}{\partial X^2} \\ \frac{\partial^2 w}{\partial Y^2} \\ 2\frac{\partial^2 w}{\partial X \partial Y} \end{Bmatrix} = \begin{Bmatrix} \frac{4}{a^2} & \frac{\partial^2 w}{\partial \xi^2} \\ \frac{4}{b^2} & \frac{\partial^2 w}{\partial \eta^2} \\ \frac{8}{ab} & \frac{\partial^2 w}{\partial \xi \partial \eta} \end{Bmatrix} \tag{A.19}$$

$$[K] = \begin{Bmatrix} -\frac{\partial^2 w}{\partial X^2} \\ -\frac{\partial^2 w}{\partial Y^2} \\ -2\frac{\partial^2 w}{\partial X \partial Y} \end{Bmatrix} = \begin{Bmatrix} -\frac{4}{a^2} & \frac{\partial^2 w}{\partial \xi^2} \\ -\frac{4}{b^2} & \frac{\partial^2 w}{\partial \eta^2} \\ -\frac{8}{ab} & \frac{\partial^2 w}{\partial \xi \partial \eta} \end{Bmatrix} \tag{A.20}$$

$$u = \frac{1}{4}(1-\xi)(1-\eta)u_1 + \frac{1}{4}(1+\xi)(1-\eta)u_2 + \frac{1}{4}(1+\xi)(1+\eta)u_3 + \frac{1}{4}(1-\xi)(1+\xi)u_4 \tag{A.21}$$

$$v = \frac{1}{4}(1-\xi)(1-\eta)v_1 + \frac{1}{4}(1+\xi)(1-\eta)v_2 + \frac{1}{4}(1+\xi)(1+\eta)v_3 + \frac{1}{4}(1-\xi)(1+\eta)v_4 \tag{A.21}$$

$$w = N_1 w_1 + N_2 \beta_1^1 + N_2 \beta_2^1 + N_4 w_2 + N_5 \beta_1^2 + N_6 \beta_2^2 + N_7 w_3 + N_8 \beta_1^3 + N_9 \beta_2^3 + N_{10} w_4 + N_{11} \beta_1^4 + N_{12} \beta_2^4$$

From the above $\frac{\partial u}{\partial \xi}$, $\frac{\partial u}{\partial \eta}$, $\frac{\partial v}{\partial \xi}$, $\frac{\partial v}{\partial \eta}$ can be found out and can be written as below:

$$\begin{Bmatrix} \frac{\partial u}{\partial X} \\ \\ \frac{\partial u}{\partial Y} \end{Bmatrix} = \begin{bmatrix} -\frac{1}{2a}(1-\eta) & \frac{1}{2a}(1-\eta) & \frac{1}{2a}(1+\eta) & -\frac{1}{2a}(1+\eta) \\ -\frac{1}{2b}(1-\xi) & -\frac{1}{2b}(1+\xi) & \frac{1}{2b}(1+\xi) & \frac{1}{2b}(1-\xi) \end{bmatrix} \begin{Bmatrix} u_1 \\ u_2 \\ u_3 \\ u_4 \end{Bmatrix} \tag{A.22}$$

Similarly

$$\begin{Bmatrix} \frac{\partial v}{\partial X} \\ \\ \frac{\partial v}{\partial Y} \end{Bmatrix} = \begin{bmatrix} -\frac{1}{2a}(1-\eta) & \frac{1}{2a}(1-\eta) & \frac{1}{2a}(1+\eta) & -\frac{1}{2a}(1+\eta) \\ -\frac{1}{2b}(1-\xi) & -\frac{1}{2b}(1+\xi) & \frac{1}{2b}(1+\xi) & \frac{1}{2b}(1-\xi) \end{bmatrix} \begin{Bmatrix} v_1 \\ v_2 \\ v_3 \\ v_4 \end{Bmatrix} \tag{A.23}$$

From the above

$$\{\varepsilon\} = \begin{Bmatrix} \frac{\partial u}{\partial X} \\ \\ \frac{\partial v}{\partial Y} \\ \\ \frac{\partial u}{\partial Y} + \frac{\partial v}{\partial X} - 2\frac{\partial^2 Z}{\partial X \partial Y} \quad w \end{Bmatrix} \tag{A.24}$$

$$= [B]_{SL} \{\delta\}^e$$

$$\begin{Bmatrix} \frac{\partial w}{\partial X} \\ \frac{\partial w}{\partial Y} \end{Bmatrix} = \begin{Bmatrix} \frac{2}{a} & \frac{\partial w}{\partial \xi} \\ \frac{2}{b} & \frac{\partial w}{\partial \eta} \end{Bmatrix}$$

$$= \begin{bmatrix} \frac{2}{a}\frac{\partial N_1}{\partial \xi} & \frac{2}{a}\frac{\partial N_2}{\partial \xi} & \frac{2}{a}\frac{\partial N_{12}}{\partial \xi} & \cdots & \frac{2}{a}\frac{\partial N_{12}}{\partial \xi} \\ \frac{2}{b}\frac{\partial N_1}{\partial \eta} & \frac{2}{b}\frac{\partial N_2}{\partial \eta} & \frac{2}{b}\frac{\partial N_3}{\partial \eta} & \cdots & \frac{2}{b}\frac{\partial N_{12}}{\partial \eta} \end{bmatrix} \{\delta\}^e \qquad (A.25)$$

$$\frac{\partial^2 w}{\partial \xi^2} = \frac{\partial^2 N_1}{\partial \xi^2} w_1 + \frac{\partial^2 N_2}{\partial \xi^2}\beta_1^1 + \frac{\partial^2 N_3}{\partial \xi^2}\beta_2^1 + \frac{\partial^2 N_4}{\partial \xi^2} w_2 + \frac{\partial^2 N_5}{\partial \xi^2}\beta_1^2$$
$$+ \frac{\partial^2 N_6}{\partial \xi^2}\beta_2^2 + \frac{\partial^2 N_7}{\partial \xi^2} w_3 + \frac{\partial^2 N_8}{\partial \xi^2}\beta_1^3 + \frac{\partial^2 N_9}{\partial \xi^2}\beta_2^3$$
$$+ \frac{\partial^2 N_{10}}{\partial \xi^2} w_4 + \frac{\partial^2 N_{11}}{\partial \xi^2}\beta_1^4 + \frac{\partial^2 N_{12}}{\partial \xi^2}\beta_2^4$$

$$\frac{\partial^2 w}{\partial \eta^2} = \frac{\partial^2 N_1}{\partial \eta^2} w_1 + \frac{\partial^2 N_2}{\partial \eta^2}\beta_1^1 + \frac{\partial^2 N_3}{\partial \eta^2}\beta_2^1$$
$$+ \frac{\partial^2 N_4}{\partial \eta^2} w_2 + \frac{\partial^2 N_5}{\partial \eta^2}\beta_1^2 + \frac{\partial^2 N_6}{\partial \eta^2}\beta_2^2$$
$$+ \frac{\partial^2 N_7}{\partial \eta^2} w_3 + \frac{\partial^2 N_8}{\partial \eta^2}\beta_1^3 + \frac{\partial^2 N_9}{\partial \eta^2}\beta_2^3$$

$$\frac{\partial^2 w}{\partial\xi\partial\eta} = \frac{\partial^2 N_1}{\partial\xi\partial\eta} w_1 + \frac{\partial^2 N_2}{\partial\xi\partial\eta} \beta_1^1 + \frac{\partial^2 N_3}{\partial\xi\partial\eta} \beta_2^1$$

$$+ \frac{\partial^2 N_4}{\partial\xi\partial\eta} w_2 + \frac{\partial^2 N_5}{\partial\xi\partial\eta} \beta_1^2 + \frac{\partial^2 N_6}{\partial\xi\partial\eta} \beta_2^2$$

$$+ \frac{\partial^2 N_7}{\partial\xi\partial\eta} w_3 + \frac{\partial^2 N_8}{\partial\xi\partial\eta} \beta_1^3 + \frac{\partial^2 N_9}{\partial\xi\partial\eta} \beta_2^3$$

$$+ \frac{\partial^2 N_{10}}{\partial\xi\partial\eta} w_4 + \frac{\partial^2 N_{11}}{\partial\xi\partial\eta} \beta_1^4 + \frac{\partial^2 N_{12}}{\partial\xi\partial\eta} \beta_2^4$$

From the above

$$\{\mathbf{K}\} = \begin{Bmatrix} -\frac{\partial^2 w}{\partial X^2} \\ -\frac{\partial^2 w}{\partial Y^2} \\ -2\frac{\partial^2 w}{\partial X \partial Y} \end{Bmatrix} = \begin{Bmatrix} -\frac{4}{a^2}\frac{\partial^2 w}{\partial \xi^2} \\ -\frac{4}{b^2}\frac{\partial^2 w}{\partial \eta} \\ -\frac{8}{ab}\frac{\partial^2 w}{\partial \xi \partial \eta} \end{Bmatrix}$$

can be found out, or

$$\{K\} = [B]_B \{\delta\}^e \qquad (A.27)$$

The inplane and bending stiffness matrix can be ca-lculated by using numerical integration technique.

The original double integral in cartesian coordinates has been transformed to

$$\int_{-1}^{1}\int_{-1}^{1} f(\xi,\eta)\,d\xi\,d\eta.$$

The above integral is equal to $\sum_{i=1}^{n} \sum_{j=1}^{n} H_j H_i f(a_j, b_i)$,

where H_j and H_i are the weighing coefficients, $f(a_j, b_i)$ are the values of the function at specified points (a_j, b_i) and n the number of Gauss points used. The present integration has been carried out for 6 Gaussian points.

APPENDIX B

COMPUTER INTEGRATION OF CONGRUENTLY TRANSFORMED MATRICES[+]

In the derivation of finite element expressions for stiffness or for stability matrices, certain integrals must be evaluated. Usually one of two following methods is employed for this evaluation:

(a) Analytical evaluation, which involves a considerable amount of tedious algebra.
(b) Numerical calculation, which may introduce truncation errors at an early stage of computation.

A method for the evaluation by the computer of analytical expressions for the integrals is presented. It avoids the tedious algebraic work, and it evaluates the exact analytical expressions for the integral. A FORTRAN IV program is written for the evaluation of these integrals for the stiffness of the element.

In structural analysis by finite elements usually either the displacement field or the equilibrium field is represented by a polynomial. This usually gives rise in the derivations to the following type of integral which generates the element of a matrix $A^{(0)}$:

$$A^{(0)} = \int_R B^T C B \, d R \qquad (B.1)$$

[+] A.P.Kabaila and P.Beckers (81).

The terms of matrix B consist of polynomial terms, matric C is of constant terms and R indicates the domain of integration. Sometimes under the integral one also has factors X,Y or Z or all.

In plate bending, plane stress or stability integrals, eq uation (C.1) becomes

$$A^{(0)} = \int\int_R B^T C B X^{(\gamma_X-1)} Y^{(\gamma_Y-1)} dXdY \qquad (B.2)$$

where γ_X and γ_Y are equal to or greater than 1, depending on whether there are factors of X and Y or not (in addition to those contained $B^T C B$).

The method presented is for the evaluation of equation (B.2). The method yields theanalytically exact value, except for the round-off errors, and with slight modification can be applied to problems involving triple and single integration. As an introduction to the solution of equation (B.2), consider the follow ing matrix operation with matrices of constant coefficients

$$A = B^T C B \qquad (B.3)$$

A typical element of matrix A can be written as follows

$$a_{ij} = \sum_k \sum_\ell b_{ki} C_{k\ell} b_{\ell j} \qquad (B.4)$$

where letters with subscripts are the elements of corresponding matrices. Equation (B.4) follows simply from the rules of matrix algebra, because

$$(C\ b)_{kj} = \sum_{\ell} C_{k\ell}\ b_{\ell j}$$

and

$$a_{ij} = \sum_{k} (b^T)_{ik}\ (C\ b)_{kj} = \sum_{k} b_{ki} \sum_{\ell} C_{k\ell}\ b_{\ell j}$$

$$= \sum_{k} \sum_{\ell} b_{ki}\ C_{k\ell}\ b_{\ell j}$$

q.e.d.

Expression (B.4) provides an algorithm which is very simple to programme, though it is not necessarily an efficient algorithm as far as computation time is concerned.

Equation (B.4) can be modified for the evaluation of equation (B.2), since a typical term of matrix B of equation (B.2), denoted by B_{ij}, can be written as follows:

$$B_{ij} = b_{ij}\ X^{d_{ij}}\ Y^{g_{ij}} \qquad (B.5)$$

where b_{ij} is a constant factor, generally a floating point number, and d_{ij} and g_{ij} are exponents of the two coordinates, usually fixed point numbers. The values of b_{ij}, d_{ij} and g_{ij} are the data for the purpos es of this discussion. Substituting B_{ij} in place of b_{ij} in equation (B.4) one can write the elements of B^T C B of equation (B.2) as follows:

$$(B^T\ C\ B)_{ij} = \sum_{k} \sum_{\ell} C_{k\ell}\ b_{ki}\ b_{\ell j}\ X^{(d_{ki}+d_{\ell j})}\ Y^{(g_{ki}+g_{\ell j})} \qquad (B.6)$$

Substituting equation (B.6) into (B.2) and observing that the summation can be done before integration, one obtains

$$a_{ij}^{(0)} = \sum_{k} \sum_{\ell} C_{k\ell}\ b_{ki}\ b_{\ell j} \iint_{R} X^{(d_{ki}+d_{\ell j}+\gamma_x-1)}\ Y^{(g_{ki}+g_{ij}+\gamma_y-1)}\ dx dy \tag{B.7}$$

where $a_{ij}^{(0)}$ are the elements of matrix $A^{(0)}$ of equation (B.2). Equation (B.7) is the basis of the algorithm.

The integration

$$I = \iint_{R} X^{(n-1)}\ Y^{(m-1)}\ dX\ dY \tag{B.8}$$

is easily carried out analytically where

$$\begin{aligned} n &= d_{ki} + d_{\ell j} + \gamma_X \\ m &= g_{ki} + g_{\ell j} + \gamma_Y \end{aligned} \tag{B.9}$$

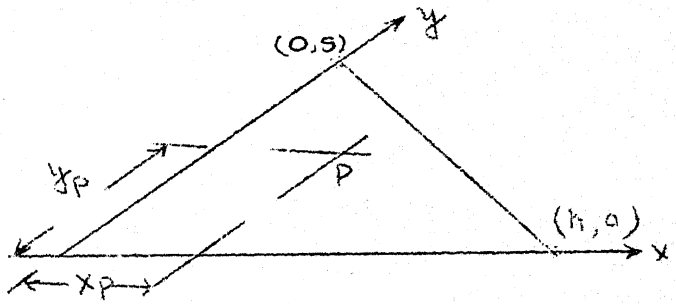

Figure B.1: Example of an integration domain.

For instance, if the domain of integration is a triangle in skew coordinates (Figure B.1), then

$$\int_0^h \int_0^S X^{(n-1)} Y^{(m-1)} \, dX dY = F(n,m) \, h^n \, S^m \qquad \text{(B.10)}$$

where

$$F(n,m) = \sum_{j=0}^{m} \binom{m}{j} \frac{(-1)^{j+1}}{m(n+j)} = \sum_{i=0}^{n} \binom{n}{i} \frac{(-1)^{i-1}}{n(m+i)} \qquad \text{(B.11)}$$

and

$$\binom{m}{j} = \frac{m(m-1) \ldots (m-j+1)}{j!}$$

Substitution of equation (B.10) into (B.7) yields)

$$a_{ij}^{(0)} = \sum_k \sum_\ell C_{k\ell} \, b_{ki} \, b_{\ell j} \, F(n,m) \, h^n \, S^M \qquad \text{(B.12)}$$

Concluding, it is seen from the example that the above greatly facilitates computer programming for the stiffness and some other matrices of finite elements. It also allows a substantial saving to be made in the analytical work associated with the programme. Furthermore, the likelihood of mistakes is greatly reduced. The co-mputer time can be greater when using this method as compared with a subroutine with algebraically evaluated and, term-by-term programmed, elements of $A^{(0)}$. This, however, is a small penalty (if any) when one is developing and testing new elements. It should be stressed that the values of $A^{(0)}$ evaluated by the method are exact, except for the rounding off errors. The truncation error, which is often encountered in numerical integration, is nonexistent in the present method.

APPENDIX C

STIFFNESS MATRIX FOR STRAIGHT BEAM WITH RESPECT TO ECCENTRIC AXES

In this appendix, the stiffness matrices for a straight beam parallel to X-axis and parallel to Y-axis respectively with respect to eccentric axes are given in tabular form. In addition to the assumption of a homogeneous, isotropic elastic material, assumptions are made which are of the same order of accuracy as those made for the shell. They are:

(1) Shear deformation is neglected (the 'Kirchhoff-Love Approximation').

(2) The beam cross-section possesses two axes of symmetry so that the shear centre coincides with the intersection of the principal axes.

Figures C.1 and C.2 show the intersection of the respective edge beams with the shell. The directions of the global axis system are clearly shown in each figure.

Tables C.1 and C.2 give the stiffness matrices of straight edge beam parallel to X-axis and Y-axis respectively with respect to eccentric axes.

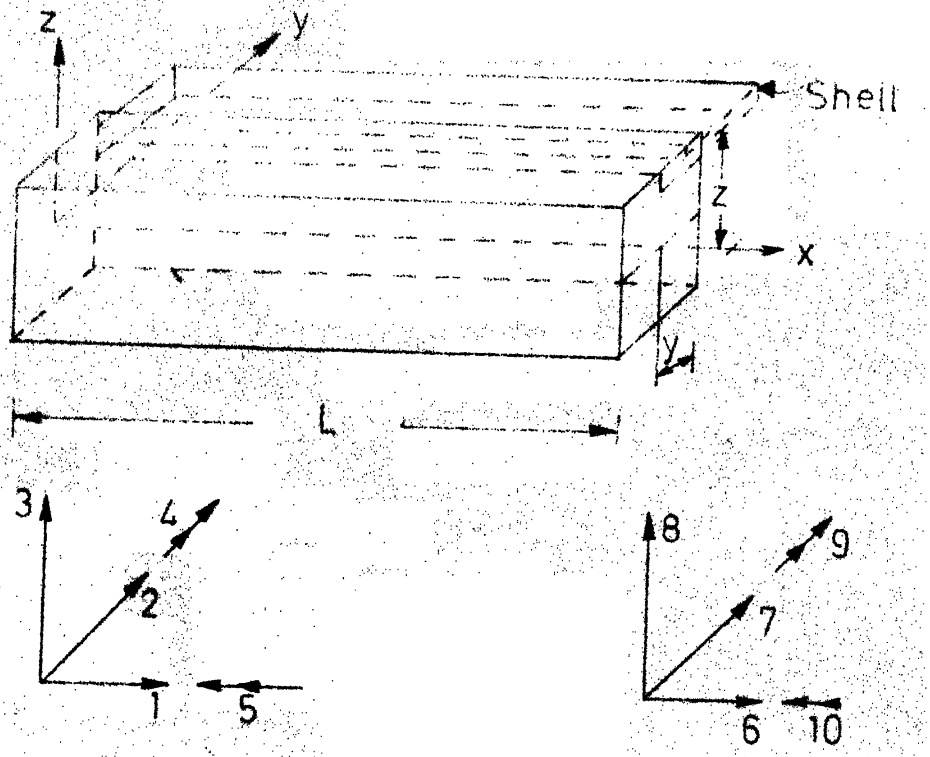

FIG. C 1 EDGE BEAM WITH AXIS PARALLEL TO x-AXIS

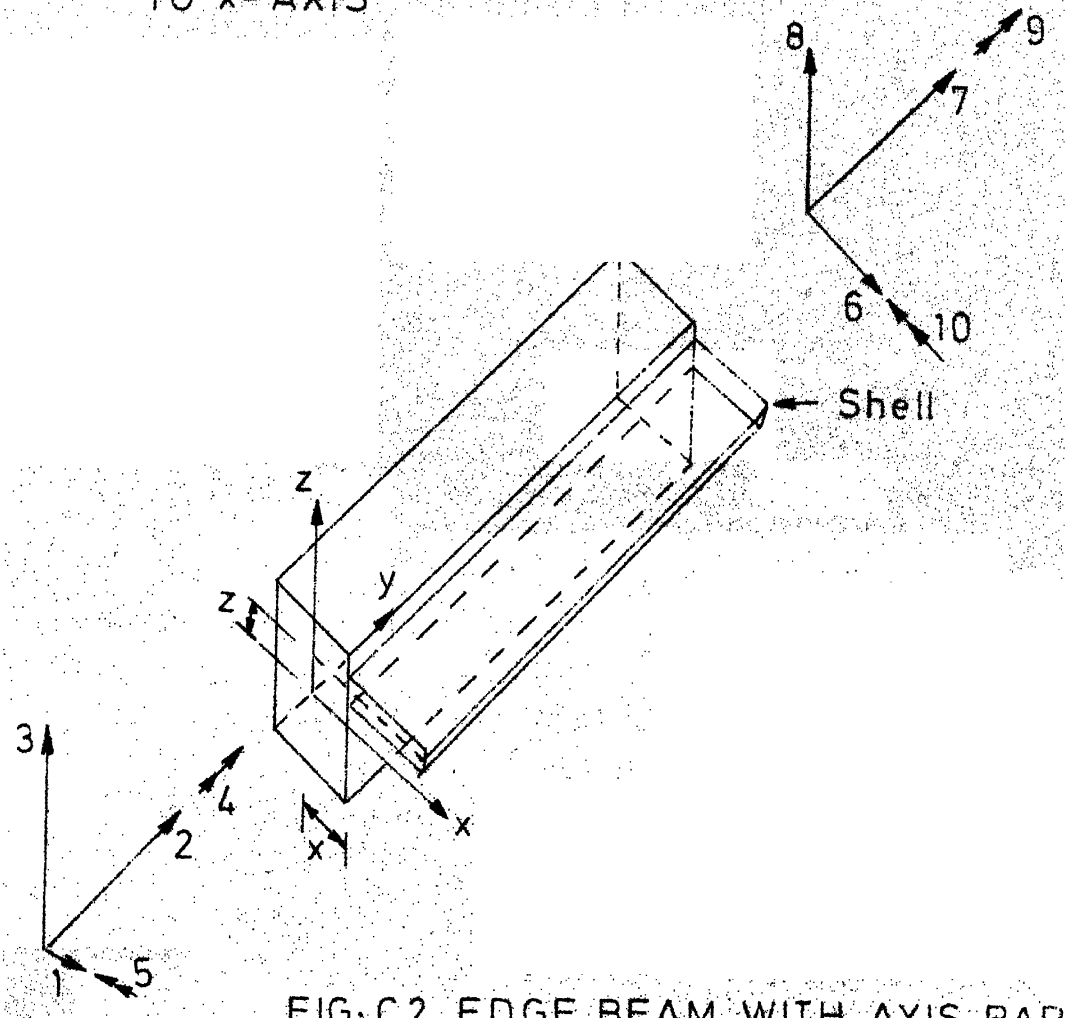

FIG. C 2 EDGE BEAM WITH AXIS PARALLEL TO y-AXIS

$\frac{EA}{L}$			$-\frac{ZEA}{L}$		$-\frac{EA}{L}$			$\frac{ZEA}{L}$	
	$\frac{12EI_Z}{L^3}$			$\frac{-12ZEI_Z}{L^3}$		$\frac{-12EI_Z}{L^3}$			$\frac{12ZEI_Z}{L^3}$
		$\frac{12EI_Y}{L^3}$	$\frac{-6EI_Y}{L^2}$	$\frac{12YEI_Y}{L^3}$			$\frac{-12EI_Y}{L^3}$	$\frac{-6EI_Y}{L^2}$	$\frac{-12YEI_Y}{L^3}$
$\frac{-ZEA}{L}$		$\frac{-6EI_Y}{L^2}$	$Z^2EA/L + 4EI_Y/L$	$\frac{-6YEI_Y}{L^2}$	$\frac{ZEA}{L}$		$\frac{6EI_Y}{L^2}$	$-Z^2EA/L + 2EI_Y/L$	$\frac{6YEI_Y}{L^2}$
	$\frac{-12ZEI_Z}{L^3}$	$\frac{12YEI_Y}{L^3}$	$\frac{-6YEI_Y}{L^2}$	$12Z^2EI_Z/L^3 + 12Y^2EI_Y/L^3 + GJ/L$		$\frac{12ZEI_Z}{L^3}$	$\frac{-12YEI_Y}{L^3}$	$\frac{-6YEI_Y}{L^2}$	$-12Z^2EI_Z/L^3 - 12Y^2EI_Y/L^3 - GJ/L$
$-\frac{EA}{L}$			$\frac{ZEA}{L}$		$\frac{EA}{L}$			$-\frac{ZEA}{L}$	
	$\frac{-12EI_Z}{L^3}$			$\frac{12ZEI_Z}{L^3}$		$\frac{12EI_Z}{L^3}$			$\frac{-12ZEI_Z}{L^3}$
		$\frac{-12EI_Y}{L^3}$	$\frac{6EI_Y}{L^2}$	$\frac{-12YEI_Y}{L^3}$			$\frac{12EI_Y}{L^3}$	$\frac{6EI_Y}{L^2}$	$\frac{12YEI_Y}{L^3}$
$\frac{ZEA}{L}$		$\frac{-6EI_Y}{L^2}$	$-Z^2EA/L + 2EI_Y/L$	$\frac{-6YEI_Y}{L^2}$	$-\frac{ZEA}{L}$		$\frac{6EI_Y}{L^2}$	$Z^2EA/L + 4EI_Y/L$	$\frac{6YEI_Y}{L^2}$
	$\frac{12ZE\ I_Z}{L^3}$	$\frac{-12YEI_Y}{L^3}$	$\frac{6YEI_Y}{L^2}$	$-12Z^2EI_Z/L^3$ $-12Y^2EI_Y/L^3$		$\frac{-12ZEI_Z}{L^3}$	$\frac{12YEI_Y}{L^3}$	$\frac{6YEI_Y}{L^2}$	$12Z^2EI_Z/L^3$

	$\frac{EA}{L}$			$-\frac{ZEA}{L}$		$-\frac{EA}{L}$			$\frac{ZEA}{L}$
		$\frac{12EI_X}{L^3}$	$\frac{12XEI_X}{L^3}$	$\frac{-6EI_X}{L^2}$			$\frac{-12EI_X}{L^3}$	$\frac{-12XEI_X}{L^3}$	$\frac{-6EI_X}{L^2}$
$\frac{-12ZEI_Z}{L^3}$		$\frac{12XEI_X}{L^3}$	$\frac{12Z^2EI_Z/L^3}{+12X^2EI_X/L^3}$ $+ GJ/L$	$\frac{-6XEI_X}{L^2}$	$\frac{12ZEI_Z}{L^3}$		$\frac{-12XEI_X}{L^3}$	$\frac{-12Z^2EI_Z/L^3}{-12X^2EI_X/L^3}$ $-GJ/L$	$\frac{-6XEI_X}{L^2}$
	$-\frac{ZEA}{L}$	$\frac{-6EI_X}{L^2}$	$\frac{-6XEI_X}{L^2}$	$Z^2EA/L +$ $4EI_X/L$		$\frac{ZEA}{L}$	$\frac{6EI_X}{L^2}$	$\frac{6XEI_X}{L^2}$	$-Z^2EA/L +$ $2EI_X/L$
$\frac{-12EI_Z}{L^3}$			$\frac{12ZEI_Z}{L^3}$		$\frac{12EI_Z}{L^3}$			$\frac{-12ZEI_Z}{L^3}$	
	$-\frac{EA}{L}$			$\frac{ZEA}{L}$		$\frac{EA}{L}$			$-\frac{ZEA}{L}$
		$\frac{-12EI_X}{L^3}$	$\frac{-12XEI_X}{L^3}$	$\frac{6EI_X}{L^2}$			$\frac{12EI_X}{L^3}$	$\frac{12XEI_X}{L^3}$	$\frac{6EI_X}{L^2}$
$\frac{12ZEI_Z}{L^3}$		$\frac{-12XEI_X}{L^3}$	$\frac{-12Z^2EI_Z/L^3}{-12X^2EI_X/L^3}$ $- GJ/L$	$\frac{6XEI_X}{L^2}$	$\frac{-12ZEI_Z}{L^3}$		$\frac{12XEI_X}{L^3}$	$\frac{12Z^2EI_Z/L^3}{+12X^2EI_X/L^3}$ $+GJ/L$	$\frac{6XEI_X}{L^2}$
	$\frac{ZEA}{L}$	$\frac{-6EI_X}{L^2}$	$\frac{-6XEI_X}{L^2}$	$-Z^2EA/L +$ $2EI_Y/L$		$-\frac{ZEA}{L}$	$\frac{6EI_X}{L^2}$	$\frac{6EI_X}{L^2}$	Z^2EA/L $+ AEI_Y/L$

APPENDIX D

SKEWED BOUNDARY CONDITIONS

In order that the skewed conditions may be treated as normal constraints, the coordinates of those nodes where skewed conditions are specified, are transformed. This transformation procedure is analogous to the transformation from local to global coordinates.

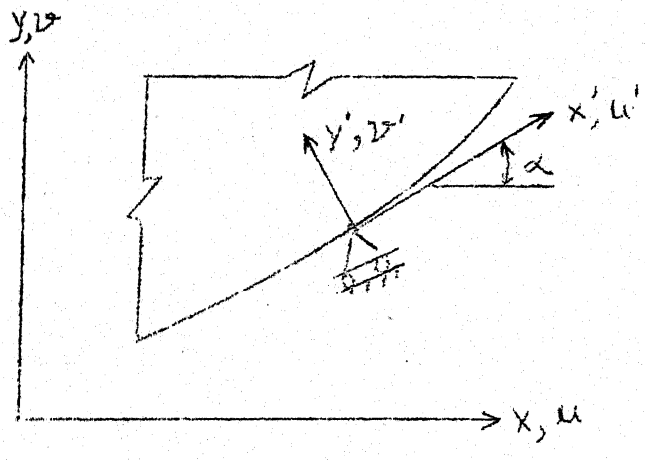

Figure D.1: Skewed Kinematic Constraint.

A prime indicates the skewed coordinate system. The transformation for displacements at the ith node as

$$\{r_i\} = [S_i]\{r_i'\} \qquad (D.1)$$

$[S_i]$ is a simple point transformation involving the direction cosines which relate the global and skewed systems. The transformation for the entire nodal displacement vector as

$$\{r\} = [S]\{r'\} \qquad (D.2)$$

Here the matrix $[S]$ is of the form

$$[S] = \begin{bmatrix} [I] & & & & \\ & [I] & & 0 & \\ & & \ddots & & \\ & & & [S_i] & \\ & 0 & & & \ddots \\ & & & & & [I] \end{bmatrix}$$

where $[I]$ is an identity matrix of the same order as $[S_i]$ and the number of submatrices on the diagonal of $[S]$ is equal to the number of nodes in the ass emblage. It follows that the order of $[S_i)$ and $[I]$ is equal to the number of displacements degrees of freedom at each node. Note that there is one $[S_i]$ matrix in $[S]$ for each node with skewed constraints. The resulting transformations for the stiffness and loads are

$$[K'] = [S]^T [K] [S]$$

$$\{R'\} = [S]^T \{R\} \qquad (D.3)$$

Note that [K]' like [K] is symmetric.

The procedure to transform skewed boundaries is often performed before the individual element stiffness and loads are assembled.